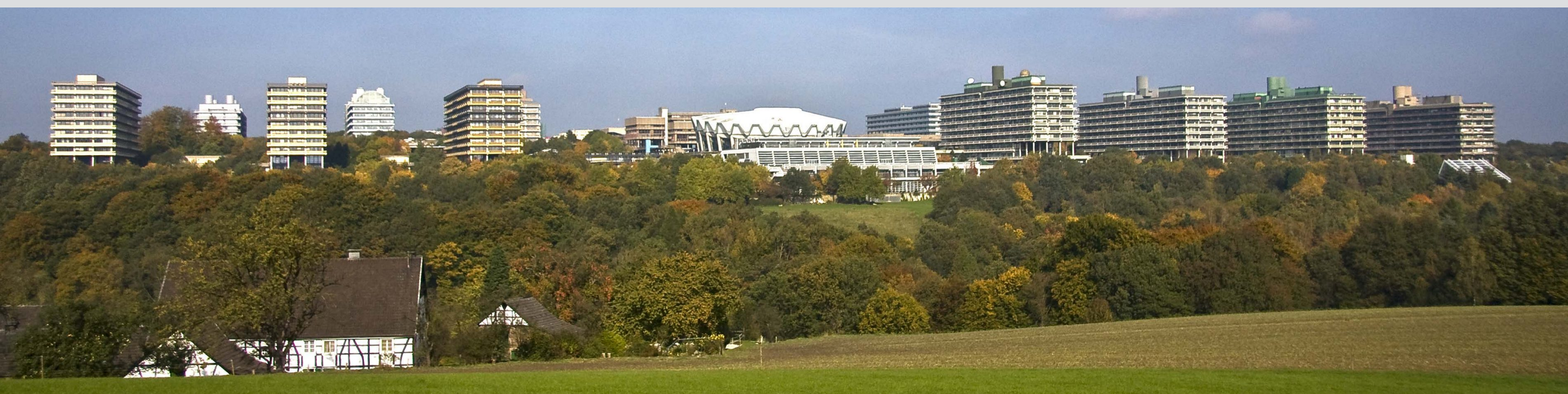
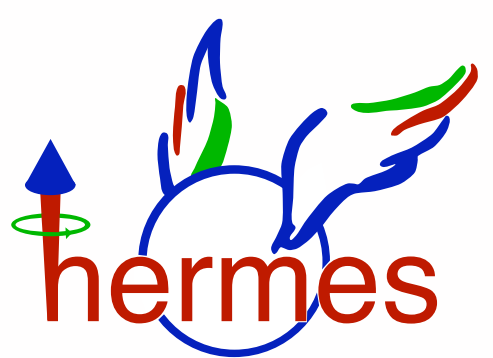


International Workshop on
Deeply Virtual Compton Scattering: From Observables to GPDs
Ruhr-Universität Bochum, February 10-12, 2014



DVCS measurements with the
 hermes recoil detector

Generalized parton distributions

- I am not supposed to explain those ...

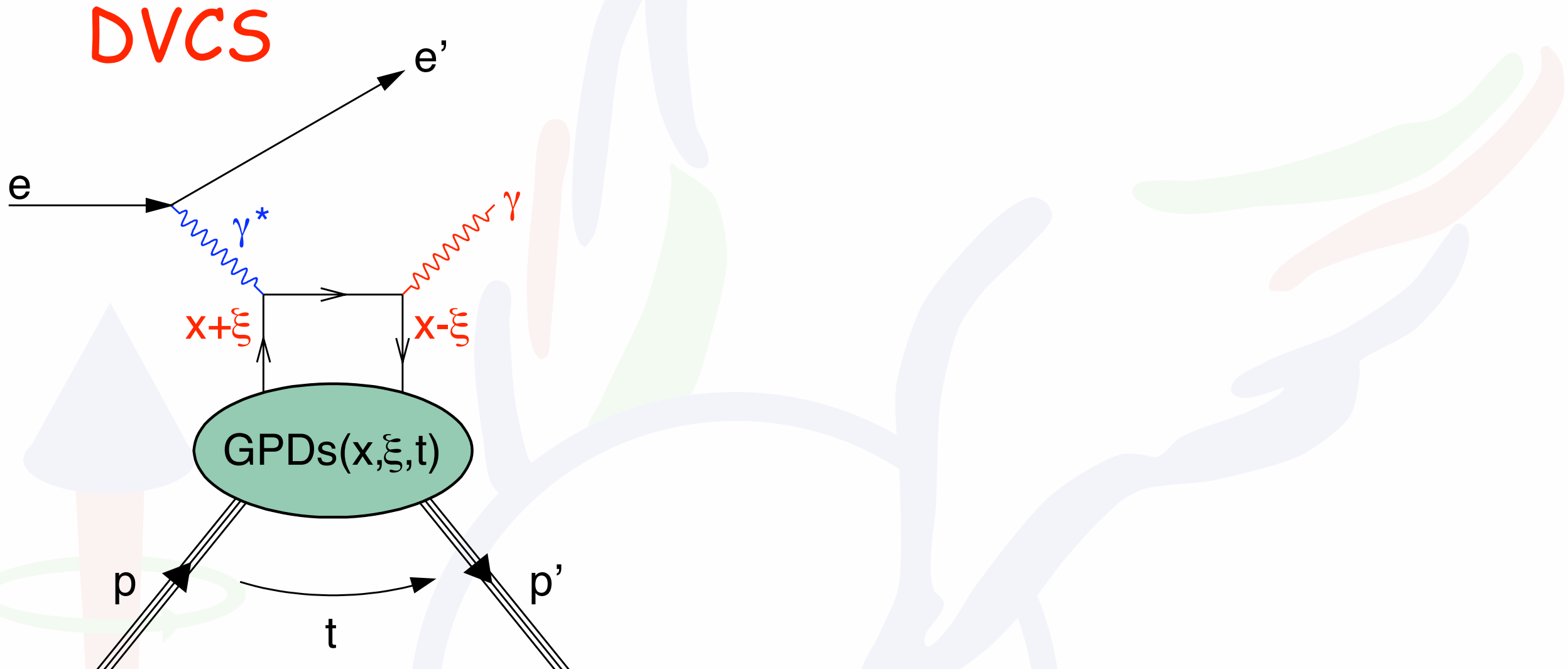


Generalized parton distributions

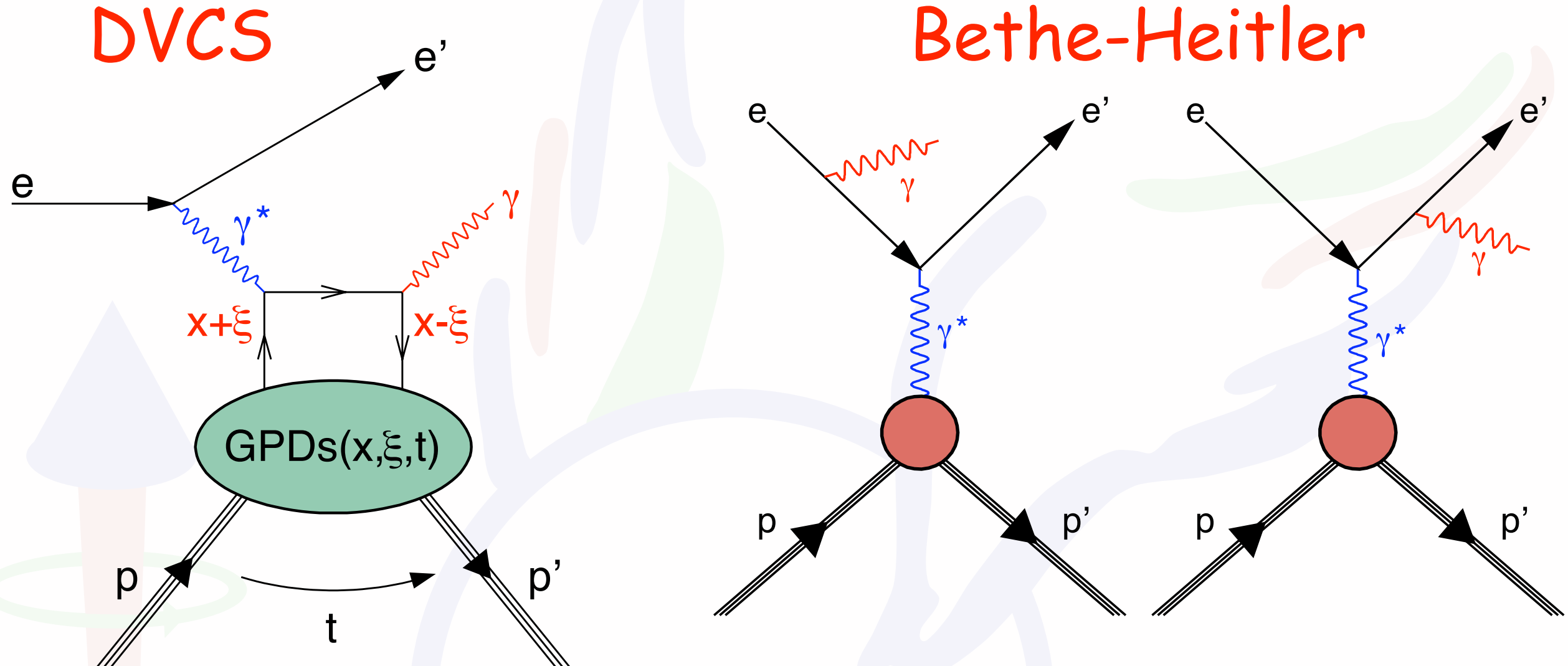
- I am not supposed to explain those ...

- ... thanks to E. Etzelmüller for a number of (backup) slides

Real-photon production

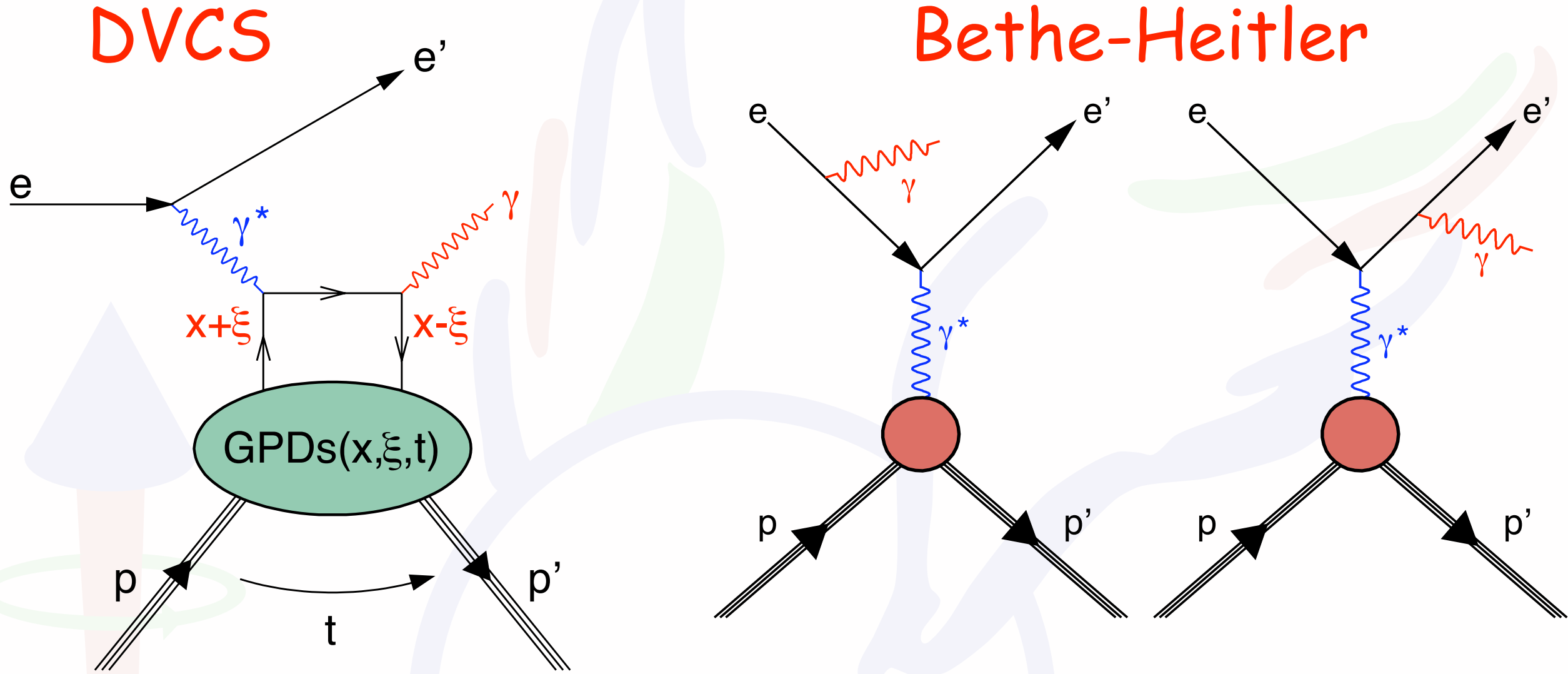


Real-photon production



$$\frac{d^4\sigma}{dQ^2 dx_B dt d\phi} = \frac{y^2}{32(2\pi)^4 \sqrt{1 + \frac{4M^2 x_B^2}{Q^2}}} (|\mathcal{T}_{\text{DVCS}}|^2 + |\mathcal{T}_{\text{BH}}|^2 + \mathcal{I})$$

Real-photon production



Amplitude of Bethe-Heitler scattering is dominant at HERMES kinematics

$$\frac{d^4\sigma}{dQ^2 dx_B dt d\phi} = \frac{y^2}{32(2\pi)^4 \sqrt{1 + \frac{4M^2 x_B^2}{Q^2}}} (|\mathcal{T}_{\text{DVCS}}|^2 + |\mathcal{T}_{\text{BH}}|^2 + \boxed{\mathcal{I}})$$

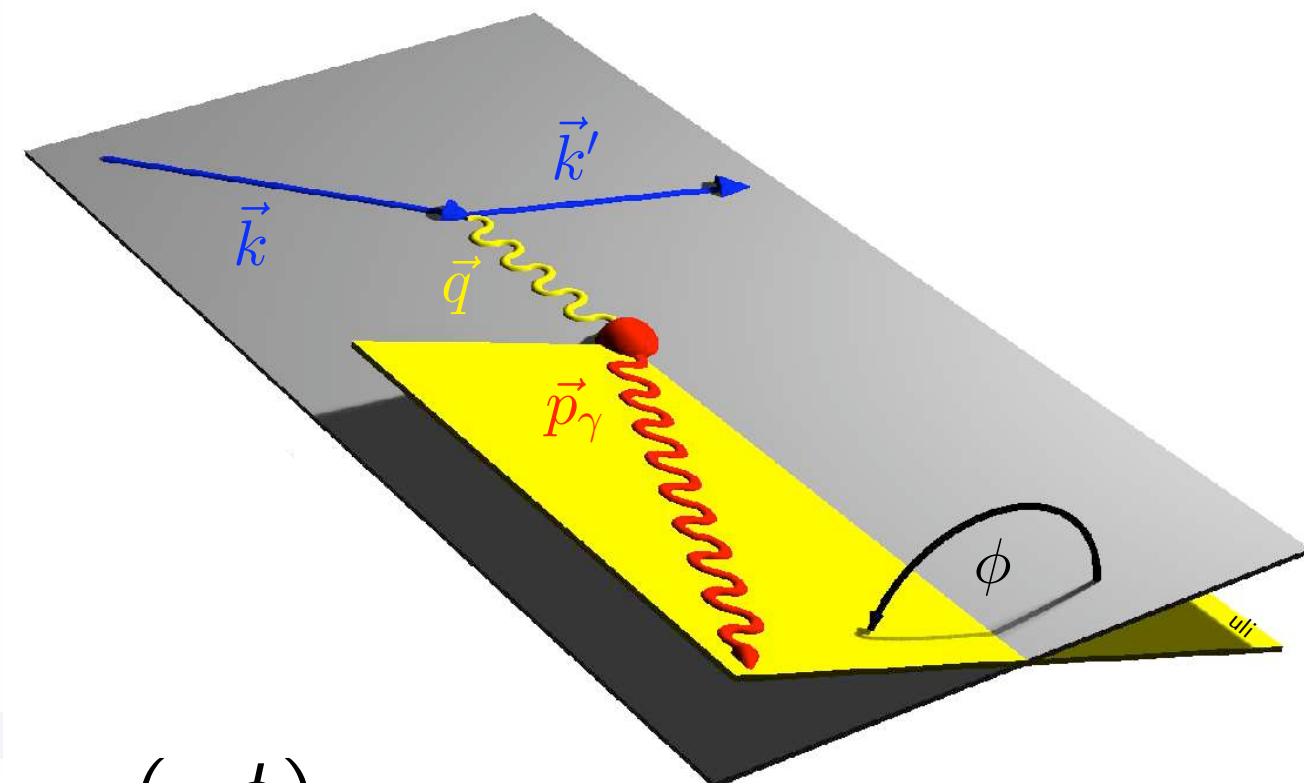
DVCS amplitude is amplified by BH in the interference term

Azimuthal dependences in DVCS/BH

- beam polarization P_B
- beam charge C_B
- here: unpolarized target

Fourier expansion for ϕ :

$$|\mathcal{T}_{\text{BH}}|^2 = \frac{K_{\text{BH}}}{\mathcal{P}_1(\phi)\mathcal{P}_2(\phi)} \sum_{n=0}^2 c_n^{\text{BH}} \cos(n\phi)$$



calculable in QED
(using FF measurements)

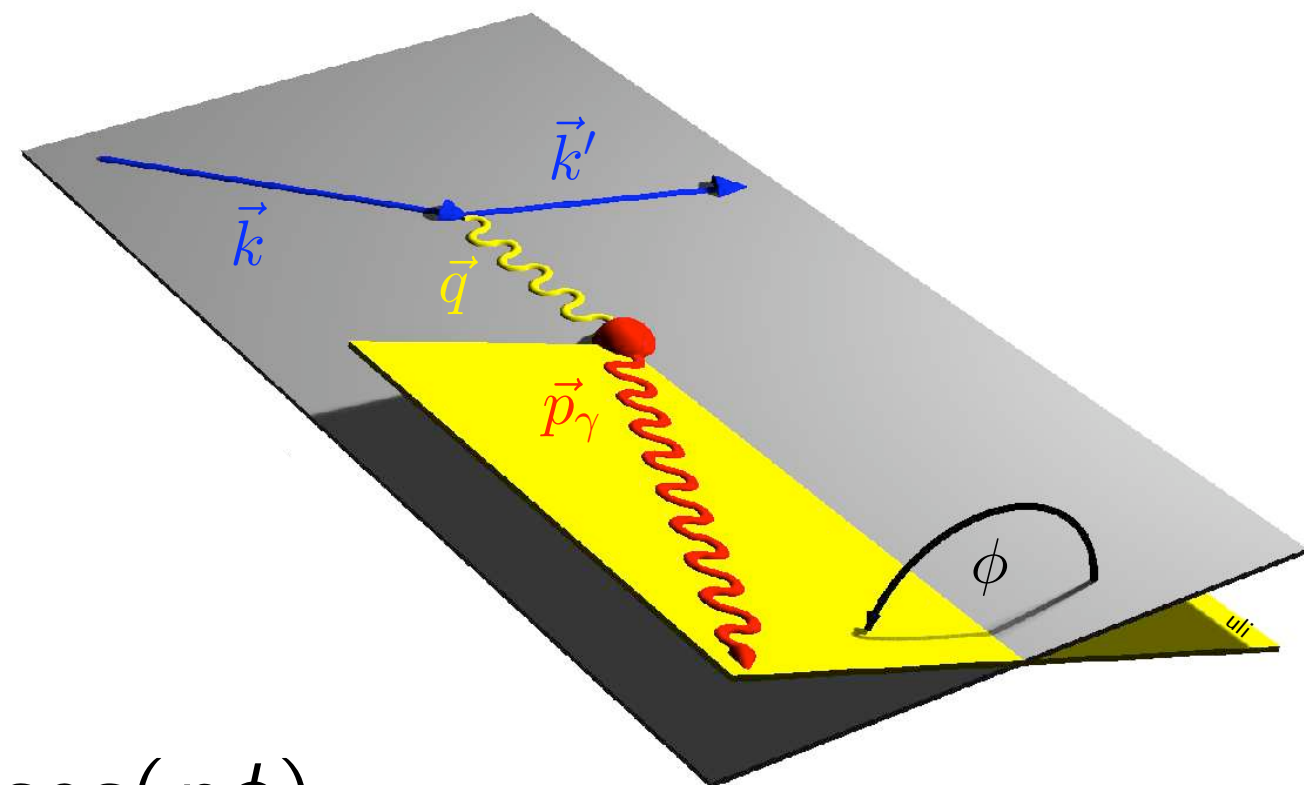
Azimuthal dependences in DVCS/BH

- beam polarization P_B
- beam charge C_B
- here: unpolarized target

Fourier expansion for ϕ :

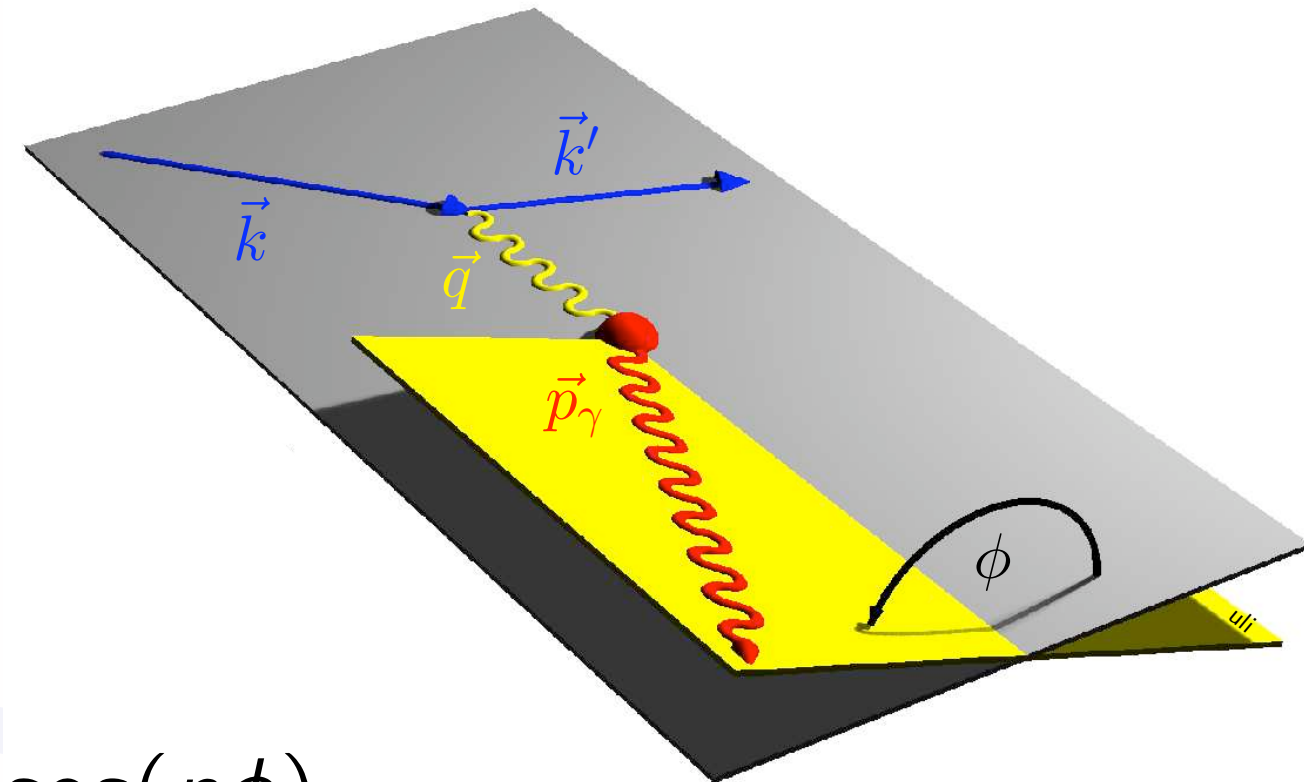
$$|\mathcal{T}_{\text{BH}}|^2 = \frac{K_{\text{BH}}}{\mathcal{P}_1(\phi)\mathcal{P}_2(\phi)} \sum_{n=0}^2 c_n^{\text{BH}} \cos(n\phi)$$

$$|\mathcal{T}_{\text{DVCS}}|^2 = K_{\text{DVCS}} \left[\sum_{n=0}^2 c_n^{\text{DVCS}} \cos(n\phi) + P_B \sum_{n=1}^1 s_n^{\text{DVCS}} \sin(n\phi) \right]$$



Azimuthal dependences in DVCS/BH

- beam polarization P_B
- beam charge C_B
- here: unpolarized target



Fourier expansion for ϕ :

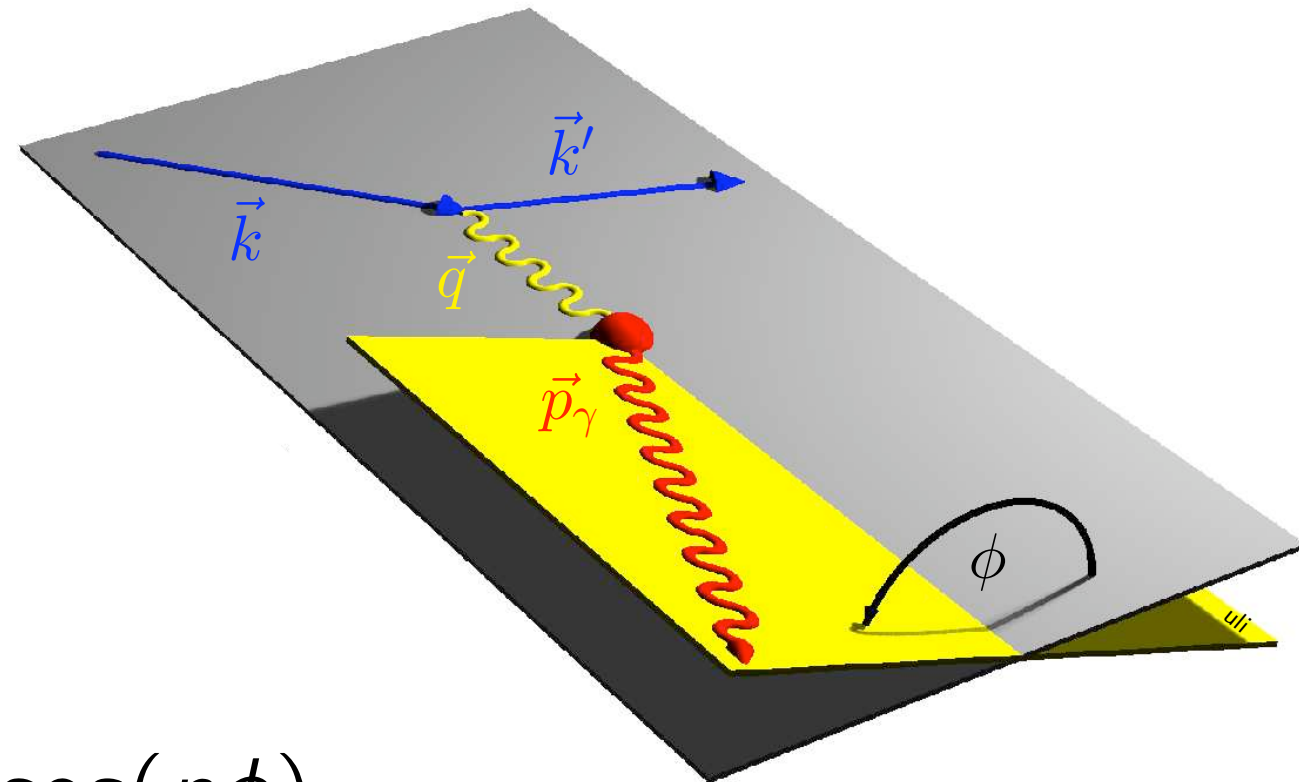
$$|\mathcal{T}_{\text{BH}}|^2 = \frac{K_{\text{BH}}}{\mathcal{P}_1(\phi)\mathcal{P}_2(\phi)} \sum_{n=0}^2 c_n^{\text{BH}} \cos(n\phi)$$

$$|\mathcal{T}_{\text{DVCS}}|^2 = K_{\text{DVCS}} \left[\sum_{n=0}^2 c_n^{\text{DVCS}} \cos(n\phi) + P_B \sum_{n=1}^1 s_n^{\text{DVCS}} \sin(n\phi) \right]$$

$$\mathcal{I} = \frac{C_B K_{\mathcal{I}}}{\mathcal{P}_1(\phi)\mathcal{P}_2(\phi)} \left[\sum_{n=0}^3 c_n^{\mathcal{I}} \cos(n\phi) + P_B \sum_{n=1}^2 s_n^{\mathcal{I}} \sin(n\phi) \right]$$

Azimuthal dependences in DVCS/BH

- beam polarization P_B
- beam charge C_B
- here: unpolarized target



Fourier expansion for ϕ :

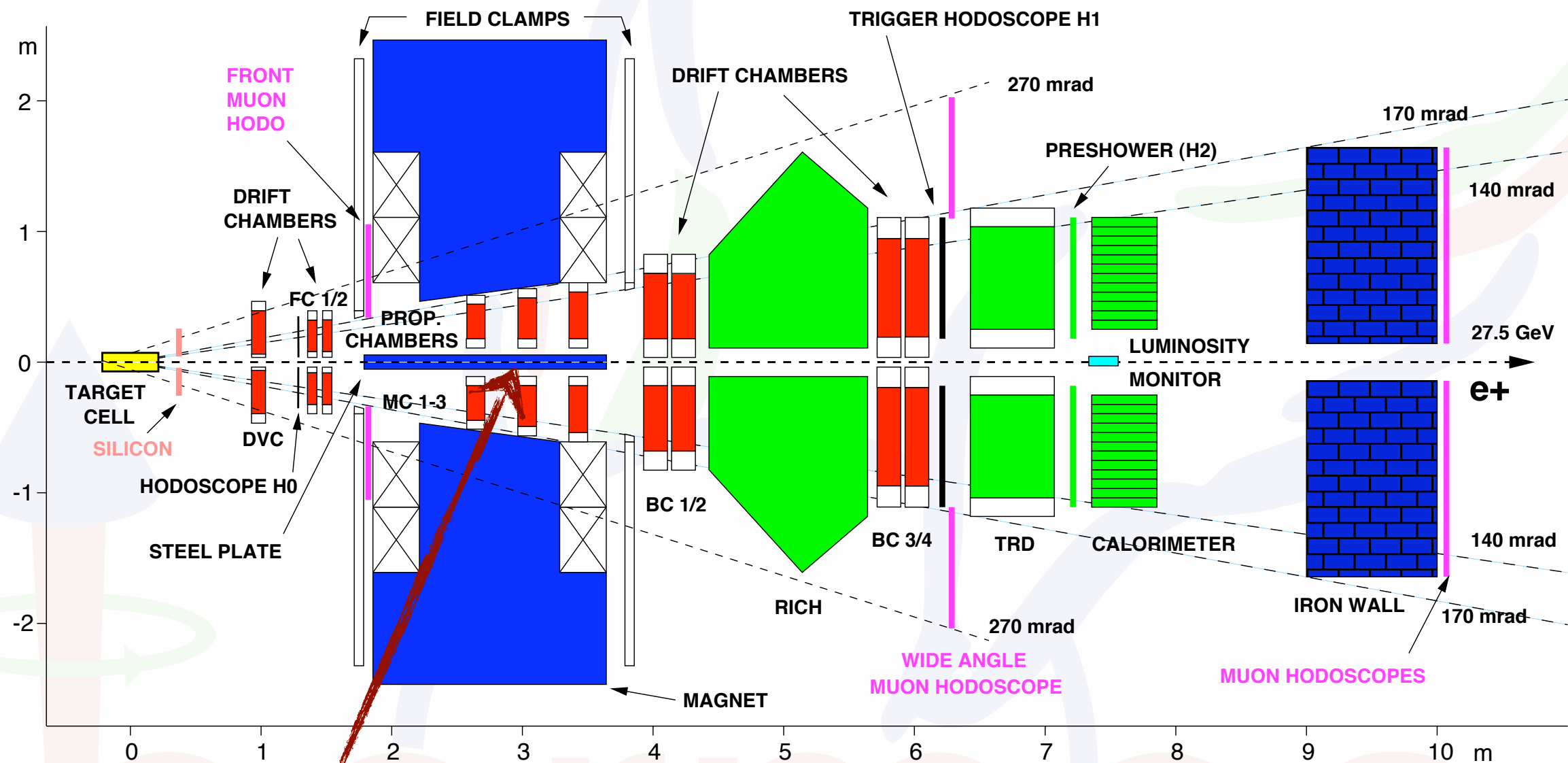
$$|\mathcal{T}_{\text{BH}}|^2 = \frac{K_{\text{BH}}}{\mathcal{P}_1(\phi)\mathcal{P}_2(\phi)} \sum_{n=0}^2 c_n^{\text{BH}} \cos(n\phi)$$

$$|\mathcal{T}_{\text{DVCS}}|^2 = K_{\text{DVCS}} \left[\sum_{n=0}^2 c_n^{\text{DVCS}} \cos(n\phi) + P_B \sum_{n=1}^1 s_n^{\text{DVCS}} \sin(n\phi) \right]$$

$$\mathcal{I} = \frac{C_B K_I}{\mathcal{P}_1(\phi)\mathcal{P}_2(\phi)} \left[\sum_{n=0}^3 c_n^I \cos(n\phi) + P_B \sum_{n=1}^2 s_n^I \sin(n\phi) \right]$$

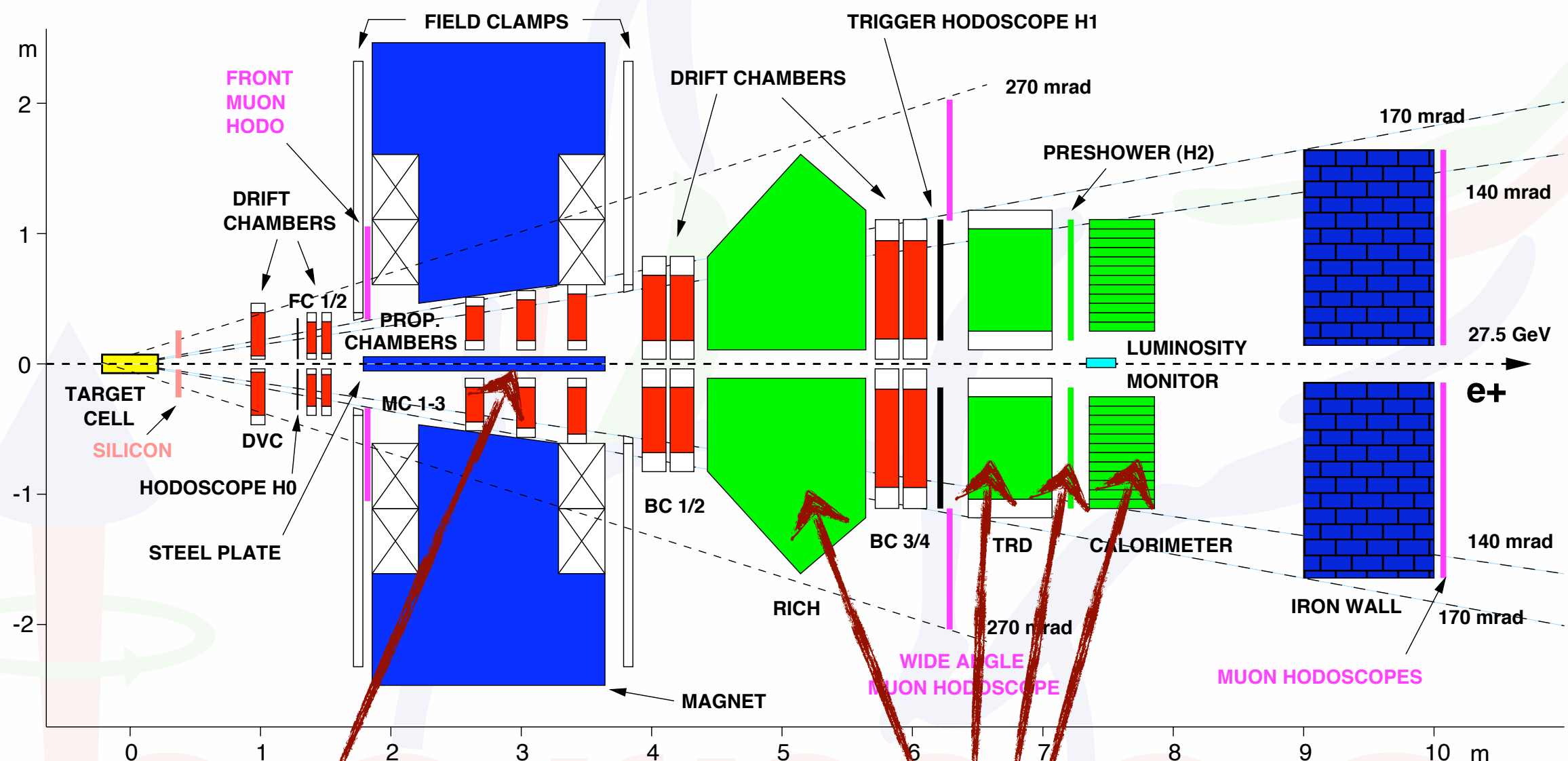
bilinear ("DVCS") or linear ("I") in GPDs

HERMES (1998-2005) schematically



two (mirror-symmetric) halves
 -> no homogenous azimuthal
 coverage

HERMES (1998-2005) schematically



two (mirror-symmetric) halves
-> no homogenous azimuthal
coverage

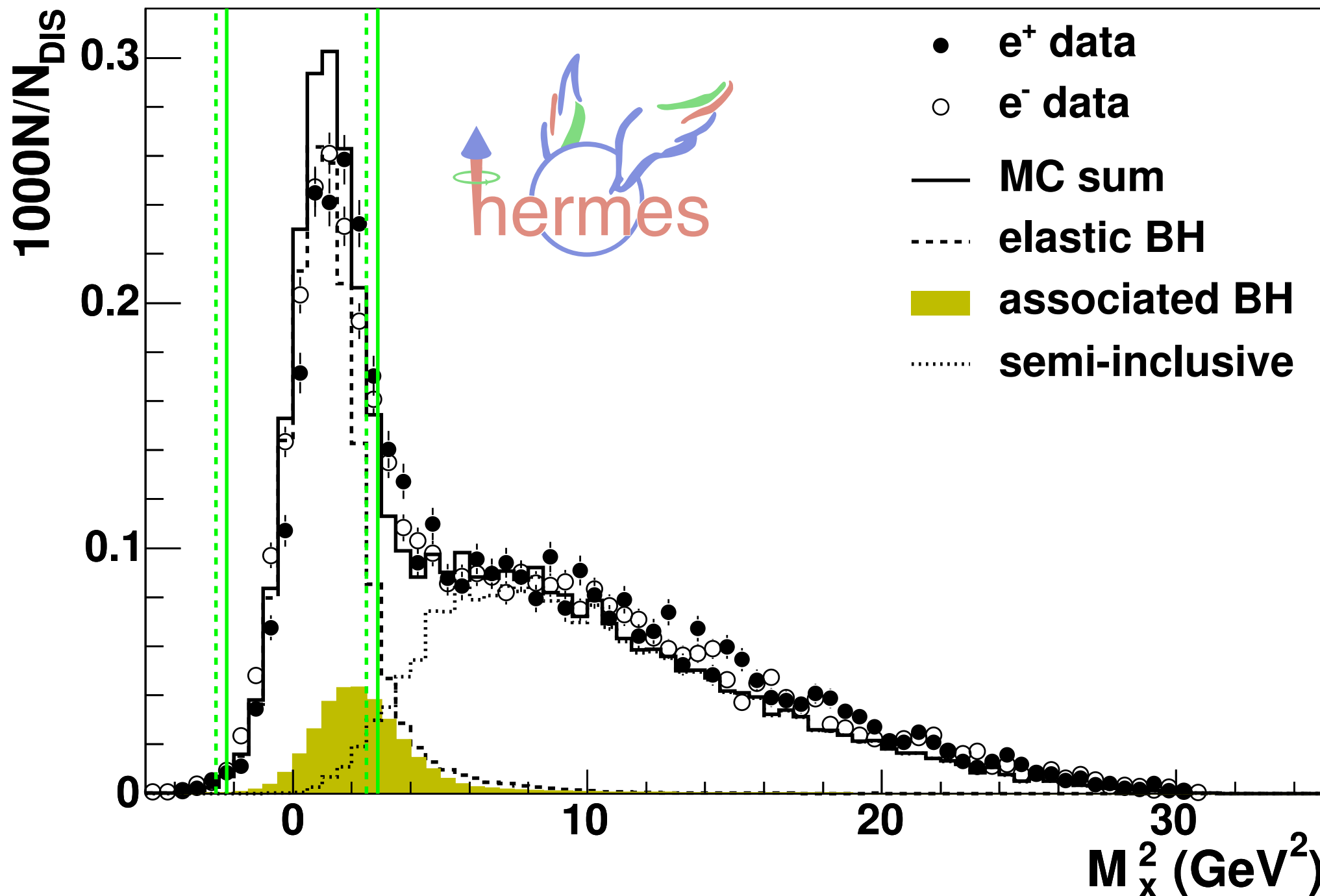
Particle ID detectors allow for

- lepton/hadron separation
- RICH: pion/kaon/proton discrimination $2\text{GeV} < p < 15\text{GeV}$

Exclusivity: missing-mass technique

$$M_x^2 = (k - k' + P_0 - P_\gamma)^2 = M^2 + 2M(\nu - E_\gamma) + t$$

ep $\rightarrow e \gamma X$

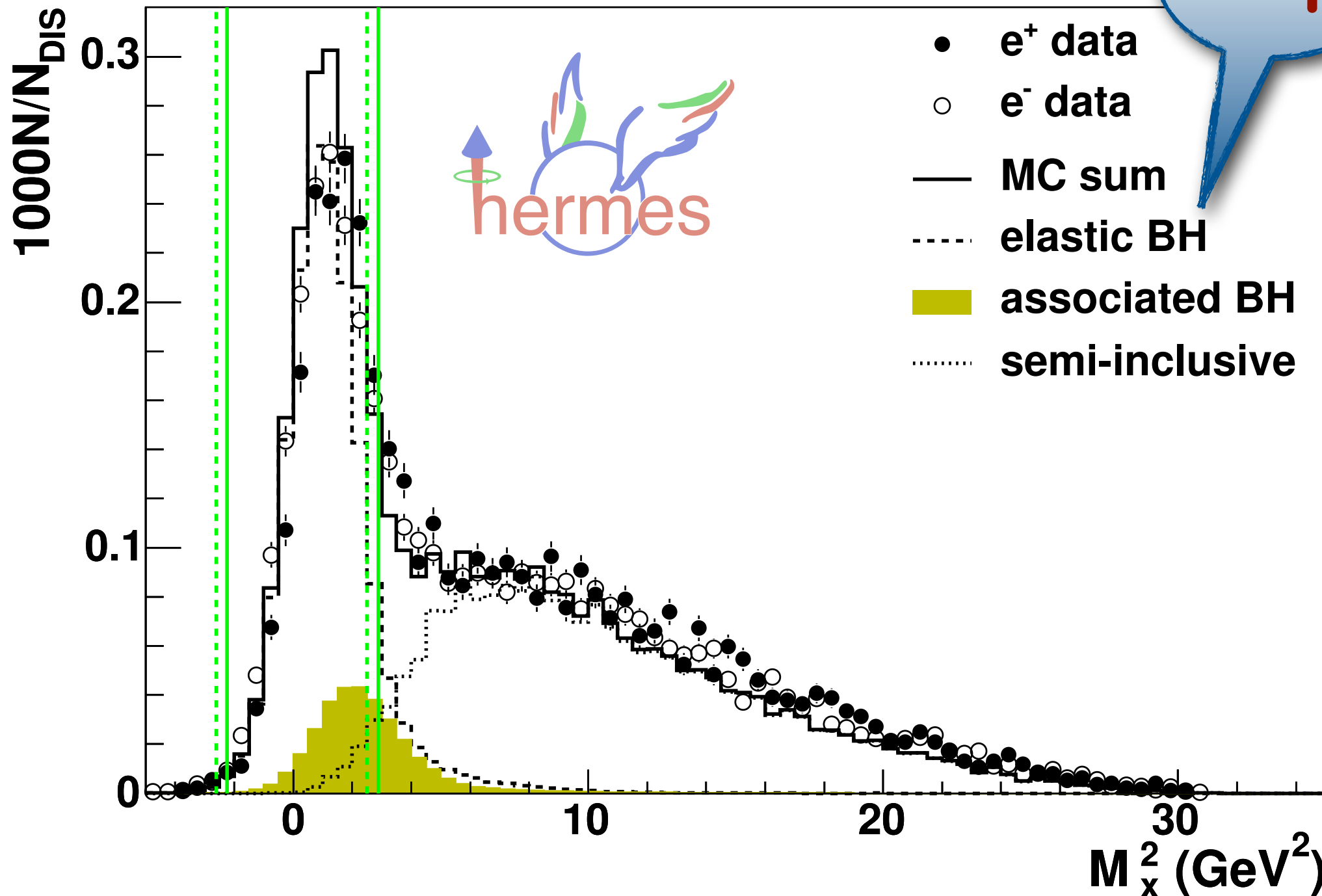


Exclusivity: missing-mass technique

$$M_x^2 = (k - k' + P_0 - P_\gamma)^2 = M^2 + 2M(\nu - E_\gamma) + t$$

$ep \rightarrow e \gamma X$

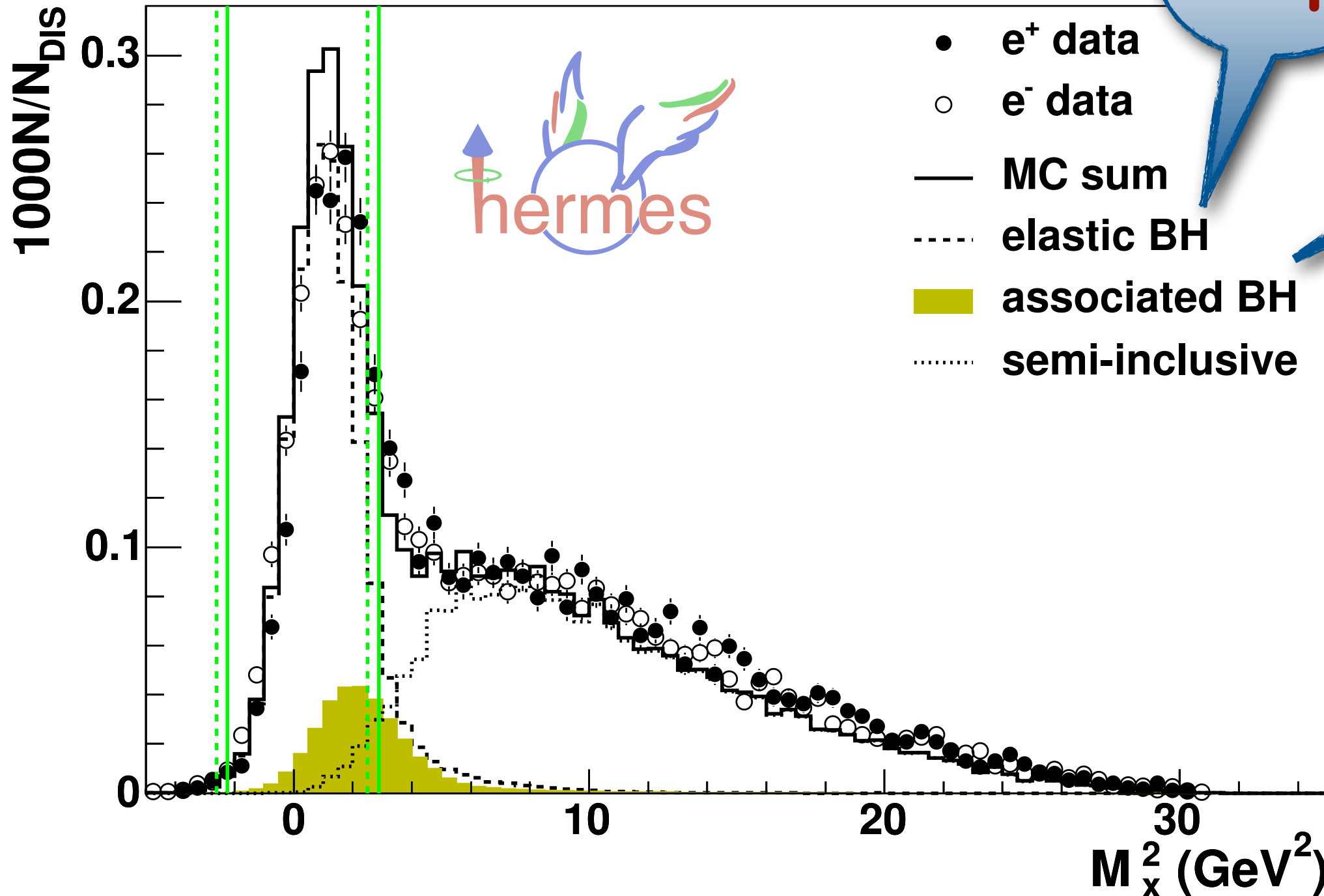
$X=p$



Exclusivity: missing-mass technique

$$M_x^2 = (k - k' + P_0 - P_\gamma)^2 = M^2 + 2M(\nu - E_\gamma) + t$$

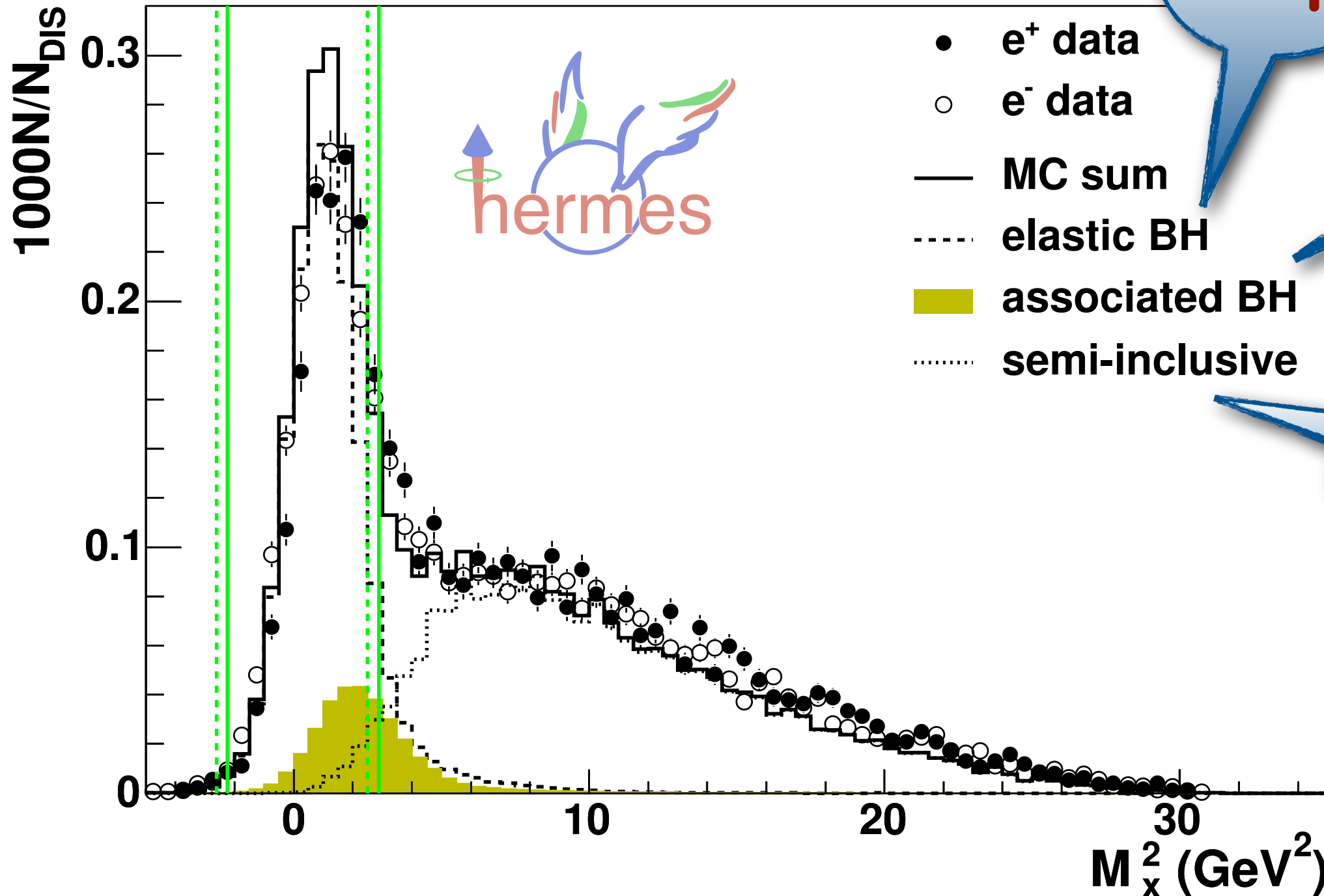
$ep \rightarrow e \gamma X$



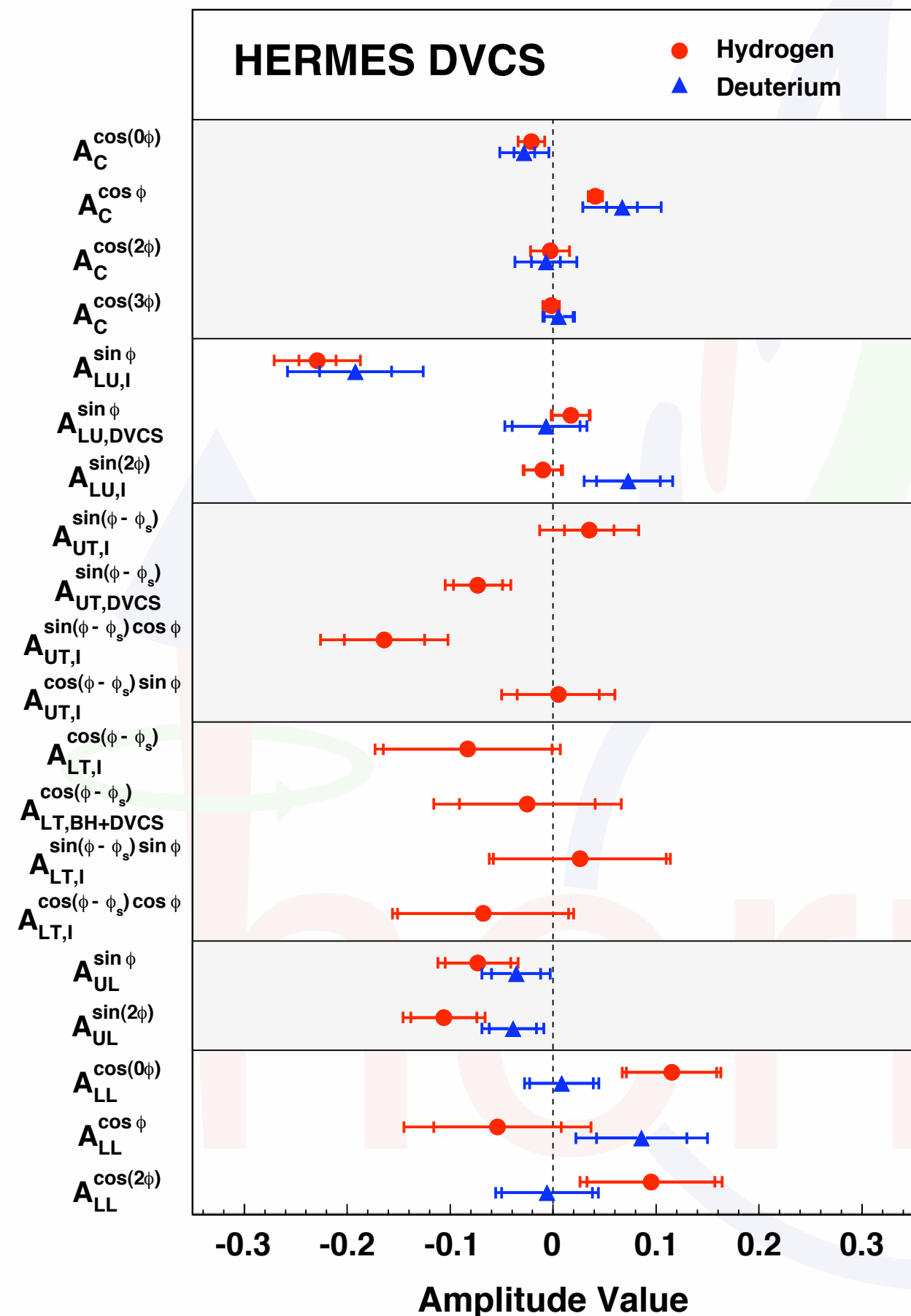
Exclusivity: missing-mass technique

$$M_x^2 = (k - k' + P_0 - P_\gamma)^2 = M^2 + 2M(\nu - E_\gamma) + t$$

$ep \rightarrow e \gamma X$



A wealth of azimuthal amplitudes



Beam-charge asymmetry:

GPD H

PRD 75 (2007) 011103

NPB 829 (2010) 1

JHEP 11 (2009) 083

PRC 81 (2010) 035202

PRL 87 (2001) 182001

JHEP 07 (2012) 032

Beam-helicity asymmetry:

GPD H

Transverse target spin asymmetries:

GPD E from proton target

JHEP 06 (2008) 066

PLB 704 (2011) 15

Longitudinal target spin asymmetry:

GPD \tilde{H}

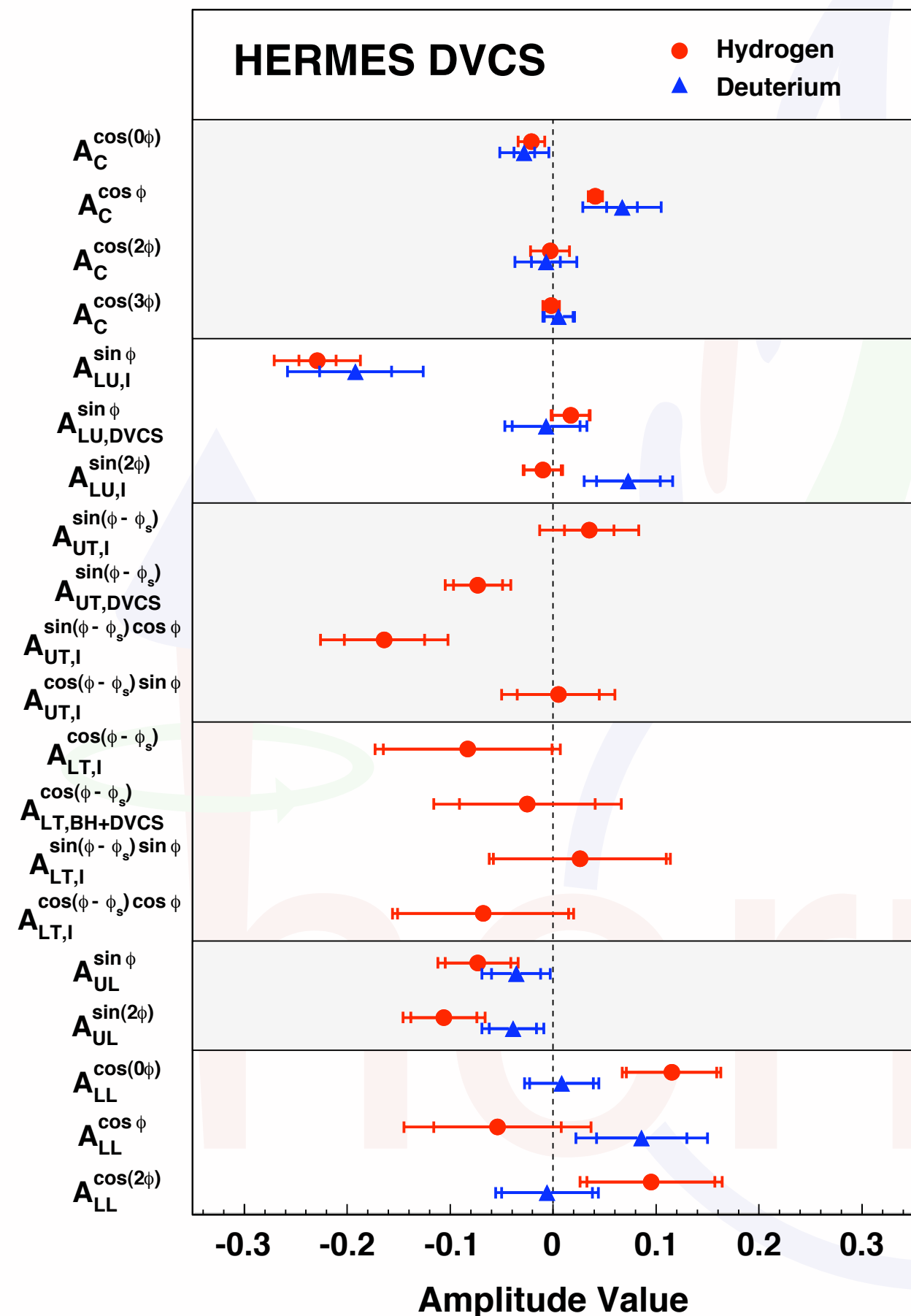
JHEP 06 (2010) 019

NPB 842 (2011) 265

Double-spin asymmetry:

GPD \tilde{H}

A wealth of azimuthal amplitudes



Beam-charge asymmetry:
GPD H

Beam-helicity asymmetry:
GPD H

Transverse target spin asymmetries:
GPD E from proton target

Longitudinal target spin asymmetry:
GPD \tilde{H}

Double-spin asymmetry:
GPD \tilde{H}

- PRD 75 (2007) 011103
- NPB 829 (2010) 1
- JHEP 11 (2009) 083
- PRC 81 (2010) 035202
- PRL 87 (2001) 182001
- JHEP 07 (2012) 032

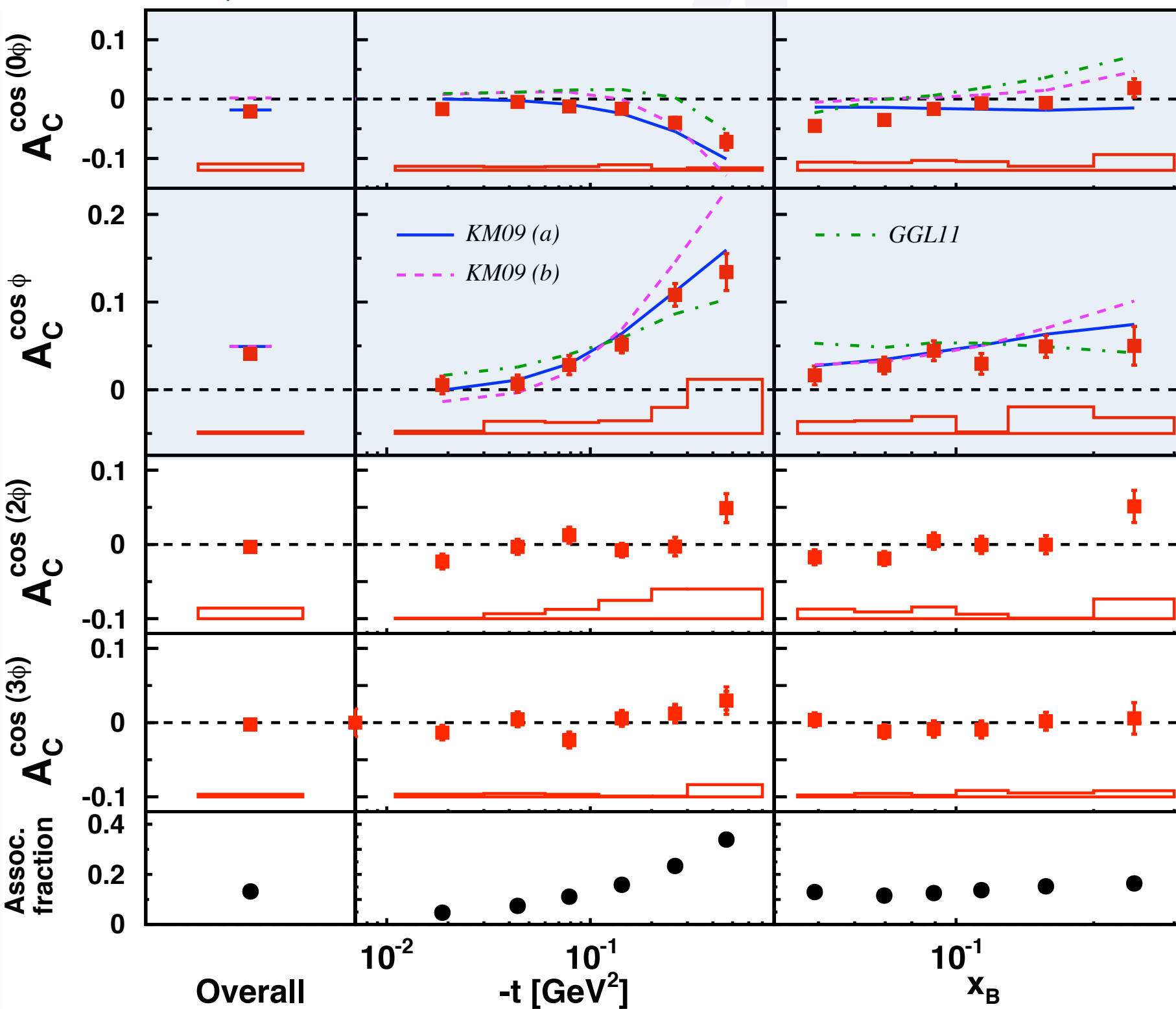
- JHEP 06 (2008) 066
- PLB 704 (2011) 15

- JHEP 06 (2010) 019
- NPB 842 (2011) 265

complete data set!

Beam-charge asymmetry

[Airapetian et al., JHEP 07 (2012) 032]



constant term:

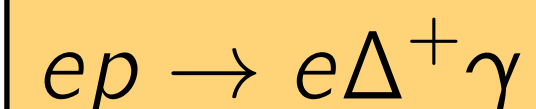
$$\propto -A_C^{\cos\phi}$$

$$\propto \text{Re}[F_1 \mathcal{H}]$$

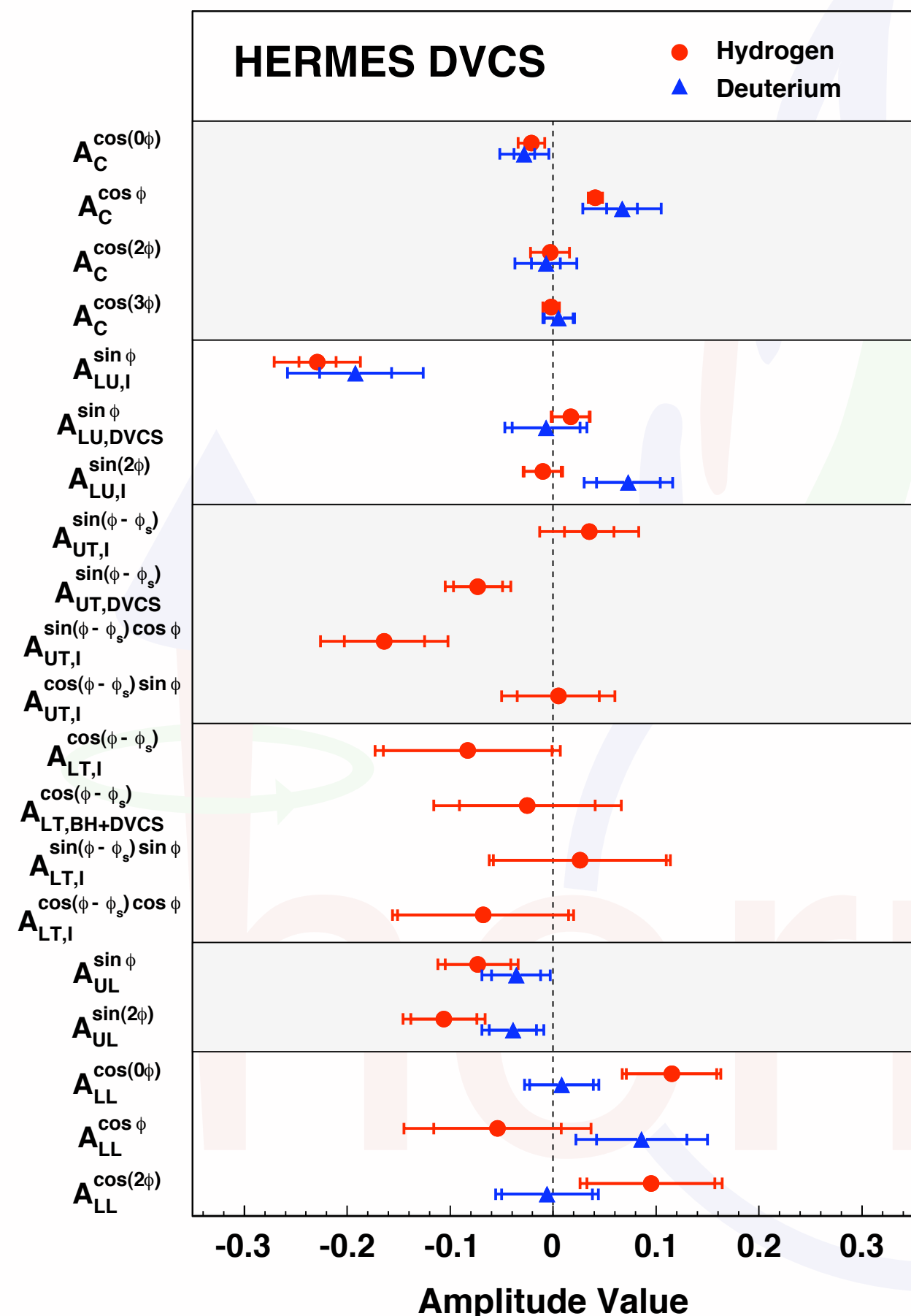
[higher twist]

[gluon leading twist]

Resonant fraction:



A wealth of azimuthal amplitudes



Beam-charge asymmetry:
GPD H

- PRD 75 (2007) 011103
- NPB 829 (2010) 1
- JHEP 11 (2009) 083
- PRC 81 (2010) 035202
- PRL 87 (2001) 182001
- JHEP 07 (2012) 032

Beam-helicity asymmetry:
GPD H

Transverse target spin asymmetries:
GPD E from proton target

- JHEP 06 (2008) 066
- PLB 704 (2011) 15

Longitudinal target spin asymmetry:
GPD \tilde{H}

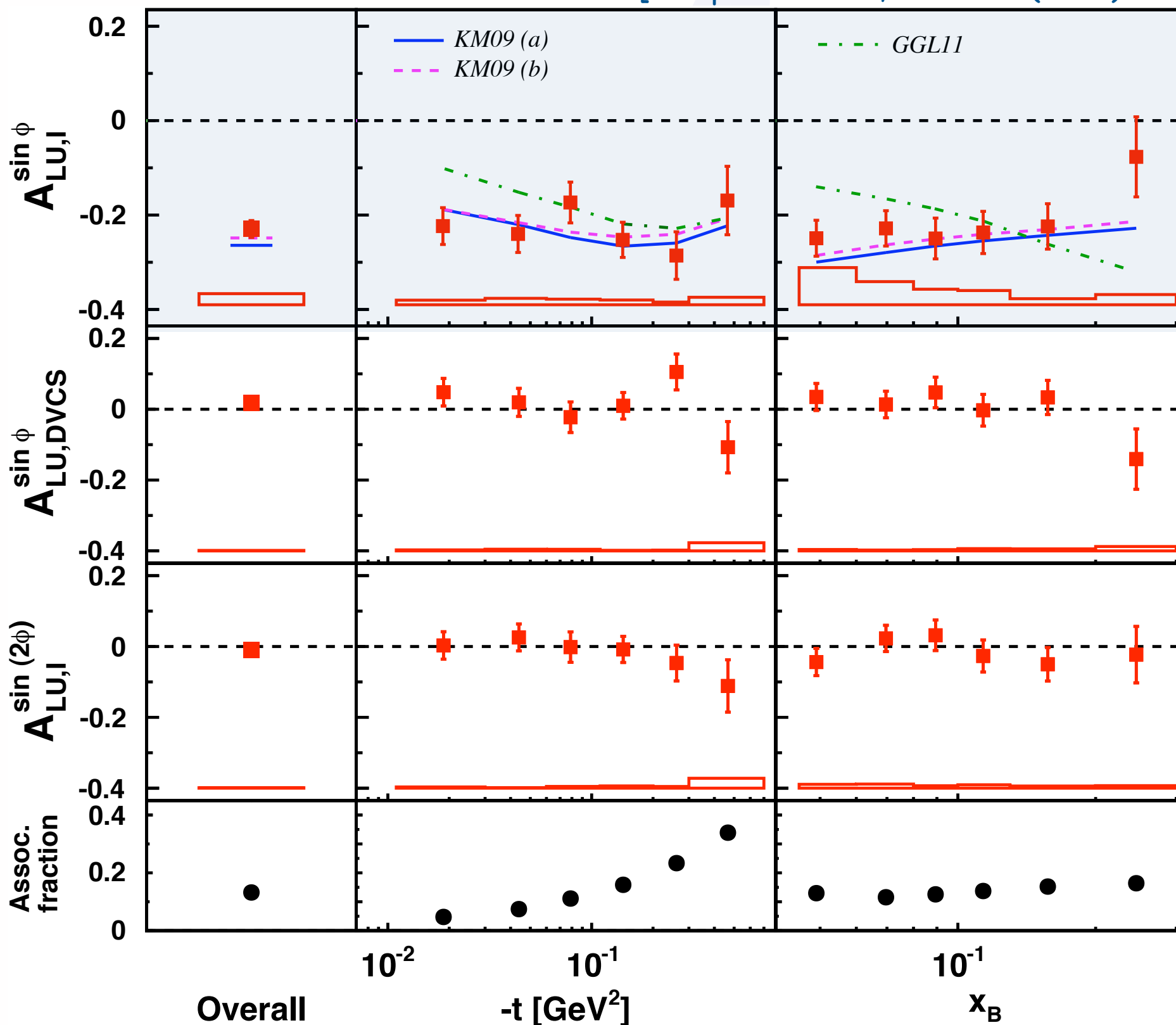
- JHEP 06 (2010) 019
- NPB 842 (2011) 265

Double-spin asymmetry:
GPD \tilde{H}

complete data set!

Beam-spin asymmetry

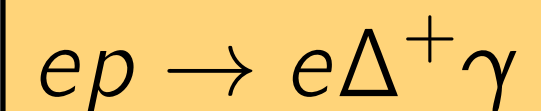
[Airapetian et al., JHEP 07 (2012) 032]



$$\propto \text{Im}[F_1 \mathcal{H}]$$

[higher twist]

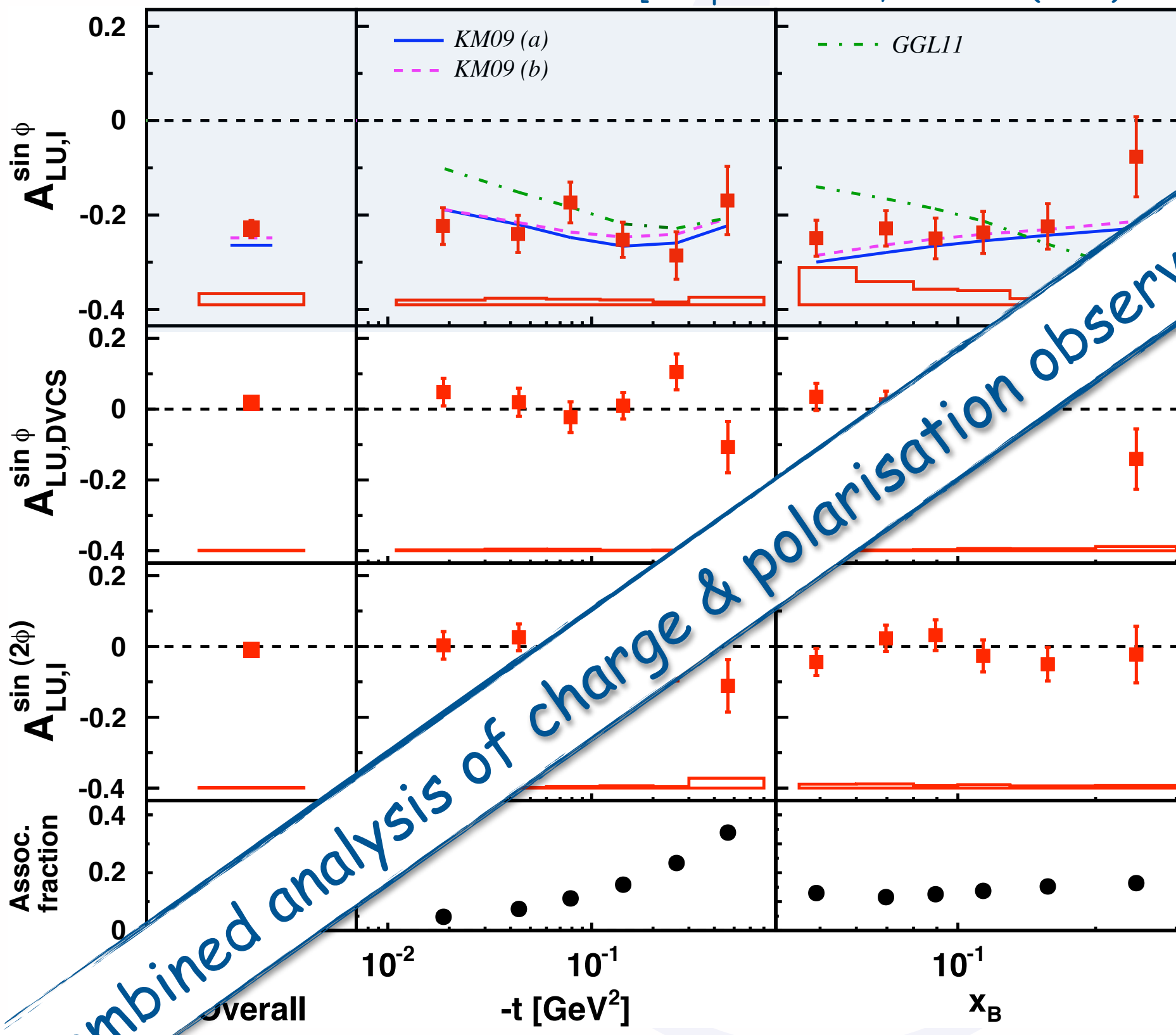
Resonant fraction:



complete data set!

Beam-spin asymmetries

[Airapetian et al., JHEP 07 (2012) 032]



gudrun.schnell @ desy.de

Combined analysis of charge & polarisation observables unique to HERA!
in $F_1 \mathcal{H}$

[higher twist]

Resonant fraction:

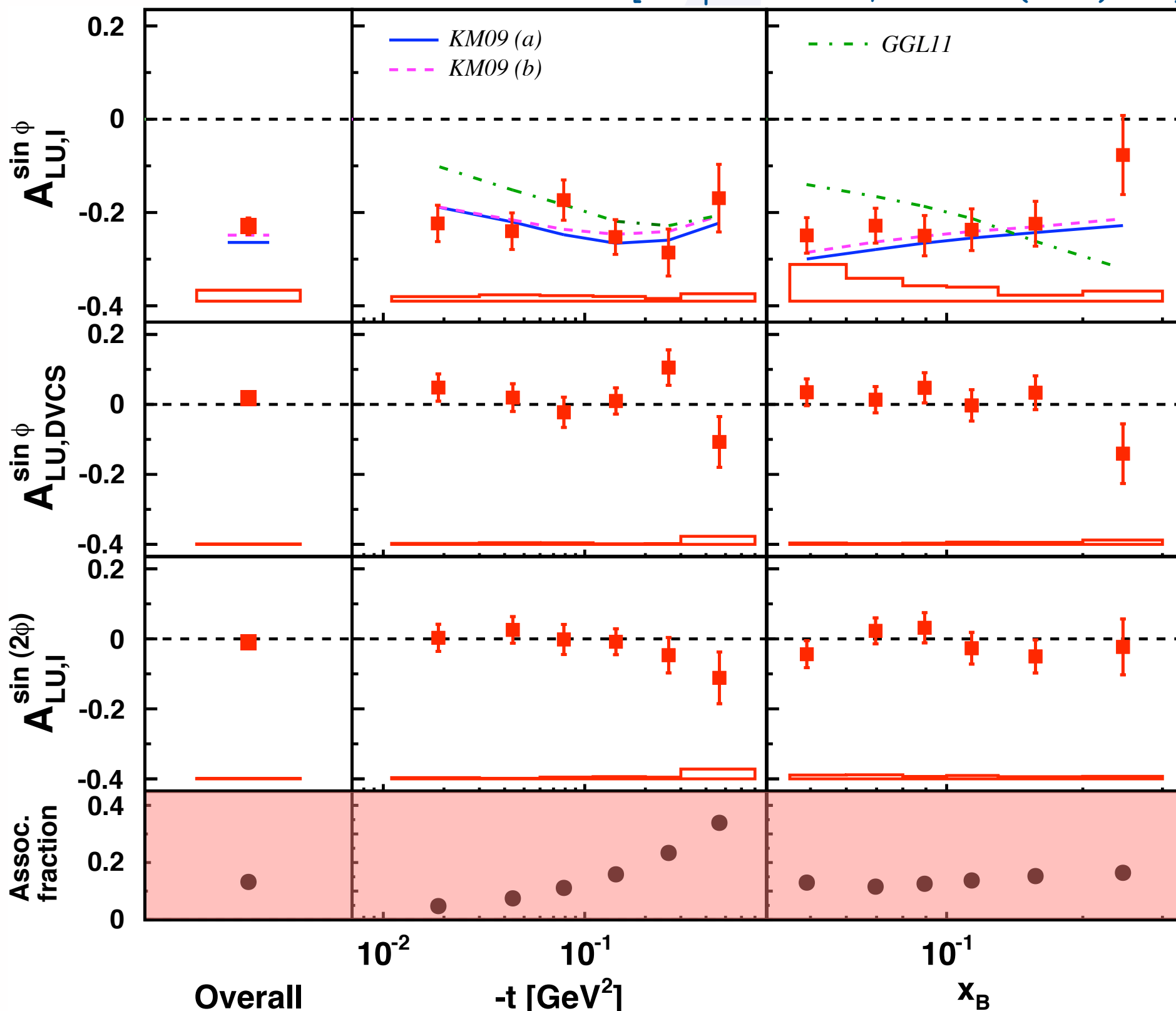
$\text{ep} \rightarrow e\Delta^+ \gamma$

DVCS 2014 - Bochum - Feb. 10th, 2014

complete data set!

Beam-spin asymmetry

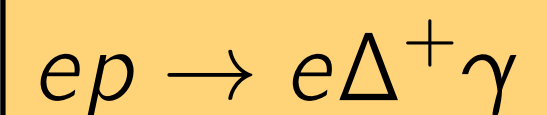
[Airapetian et al., JHEP 07 (2012) 032]



$$\propto \text{Im}[F_1 \mathcal{H}]$$

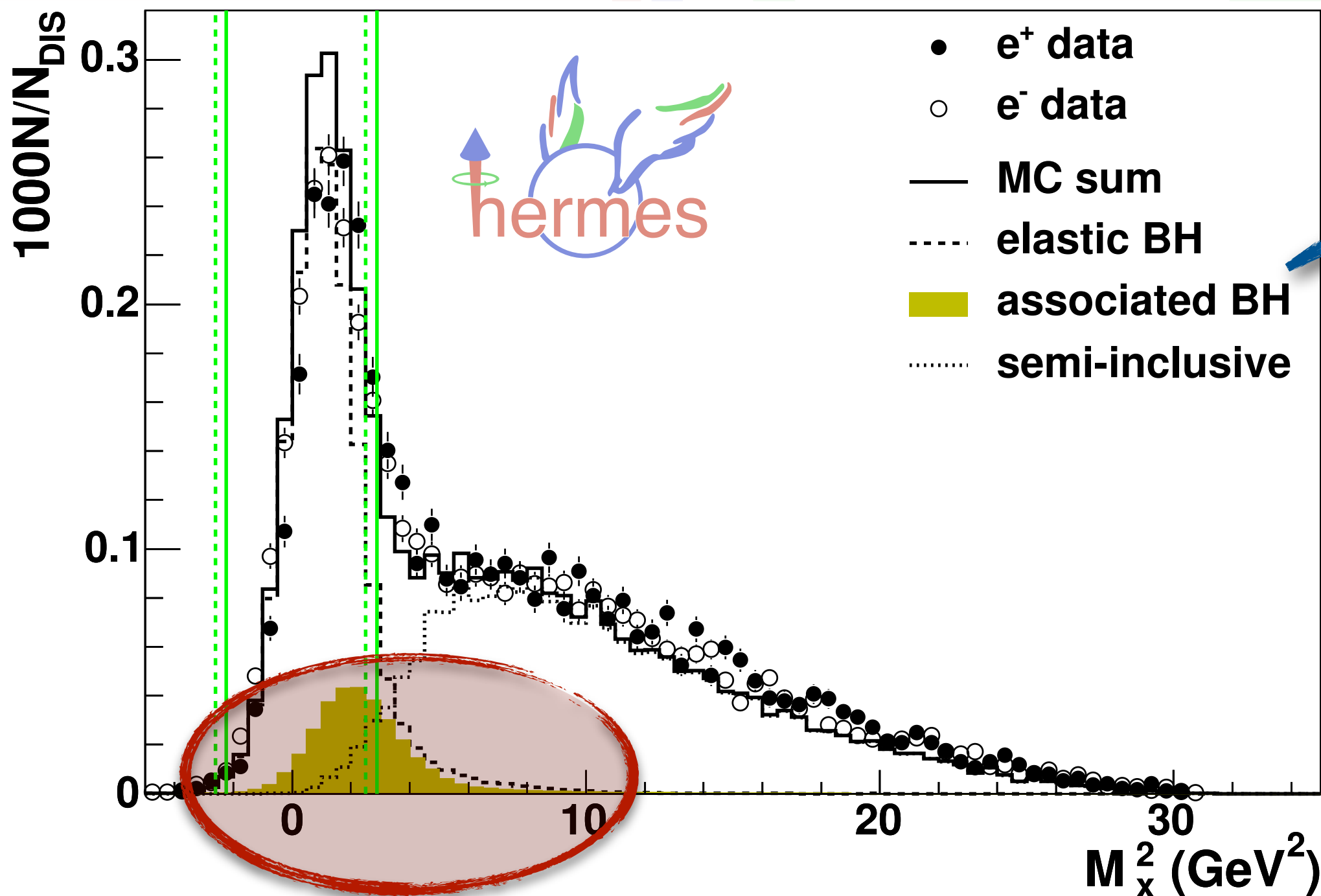
[higher twist]

Resonant fraction:



Exclusivity: missing-mass technique

$e p \rightarrow e \gamma X$

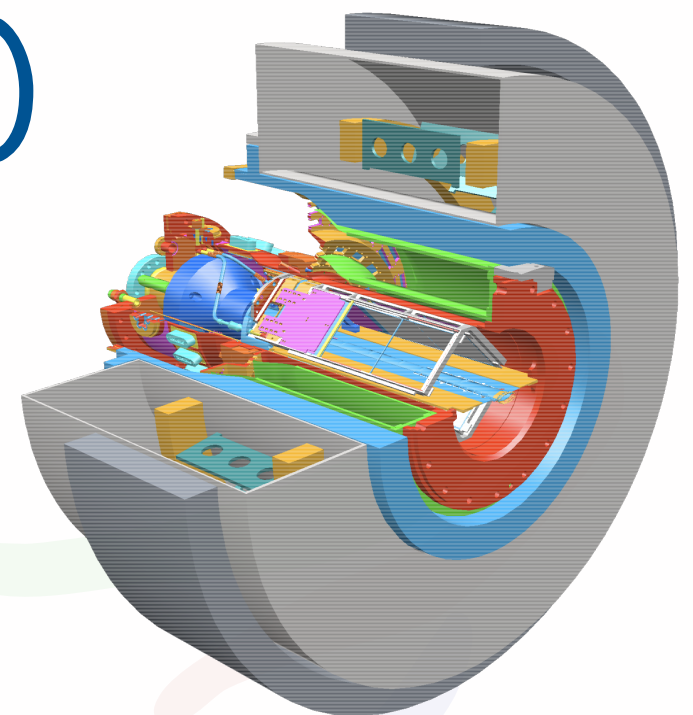
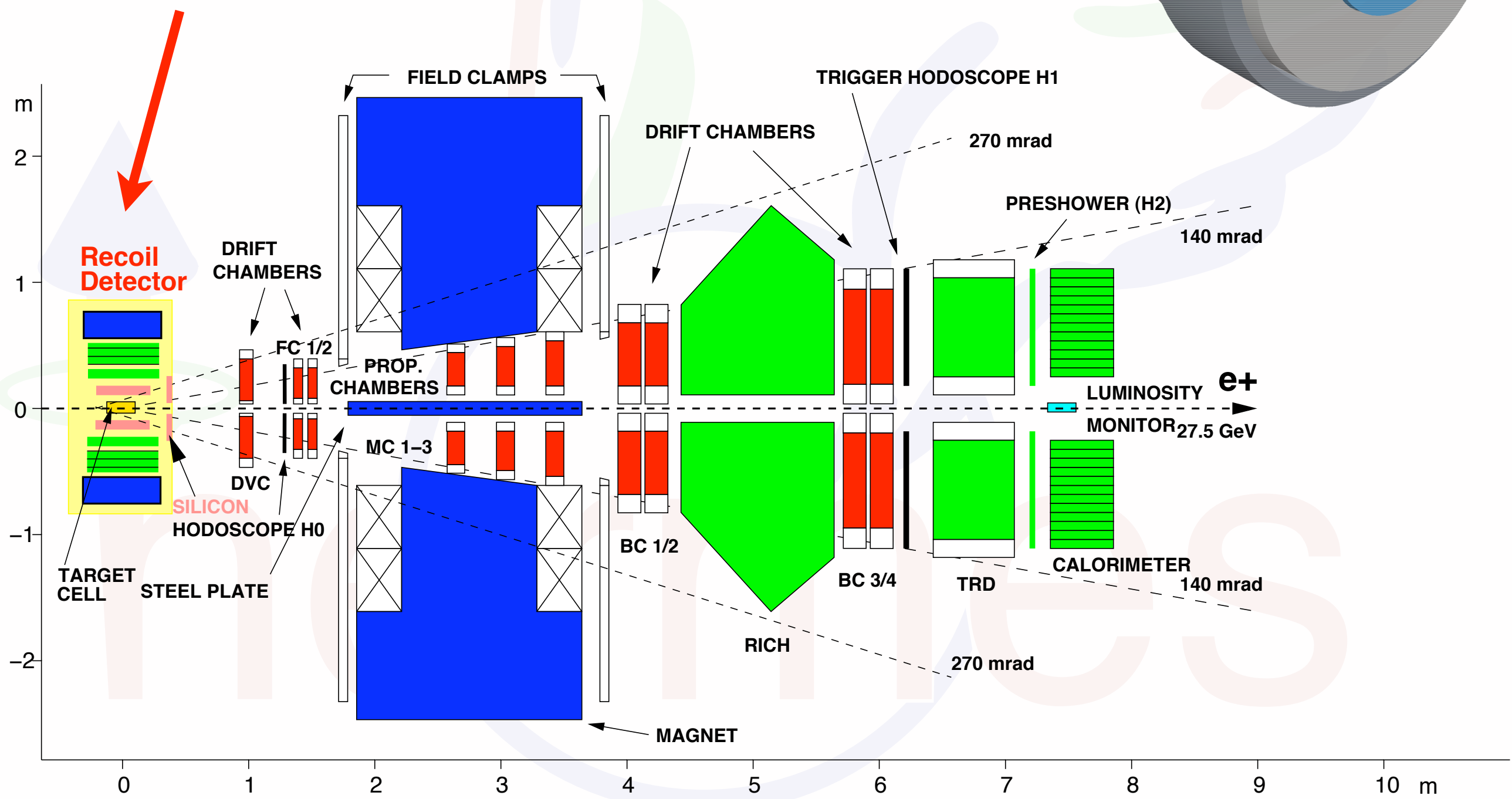


$X = \Delta^+, \dots$

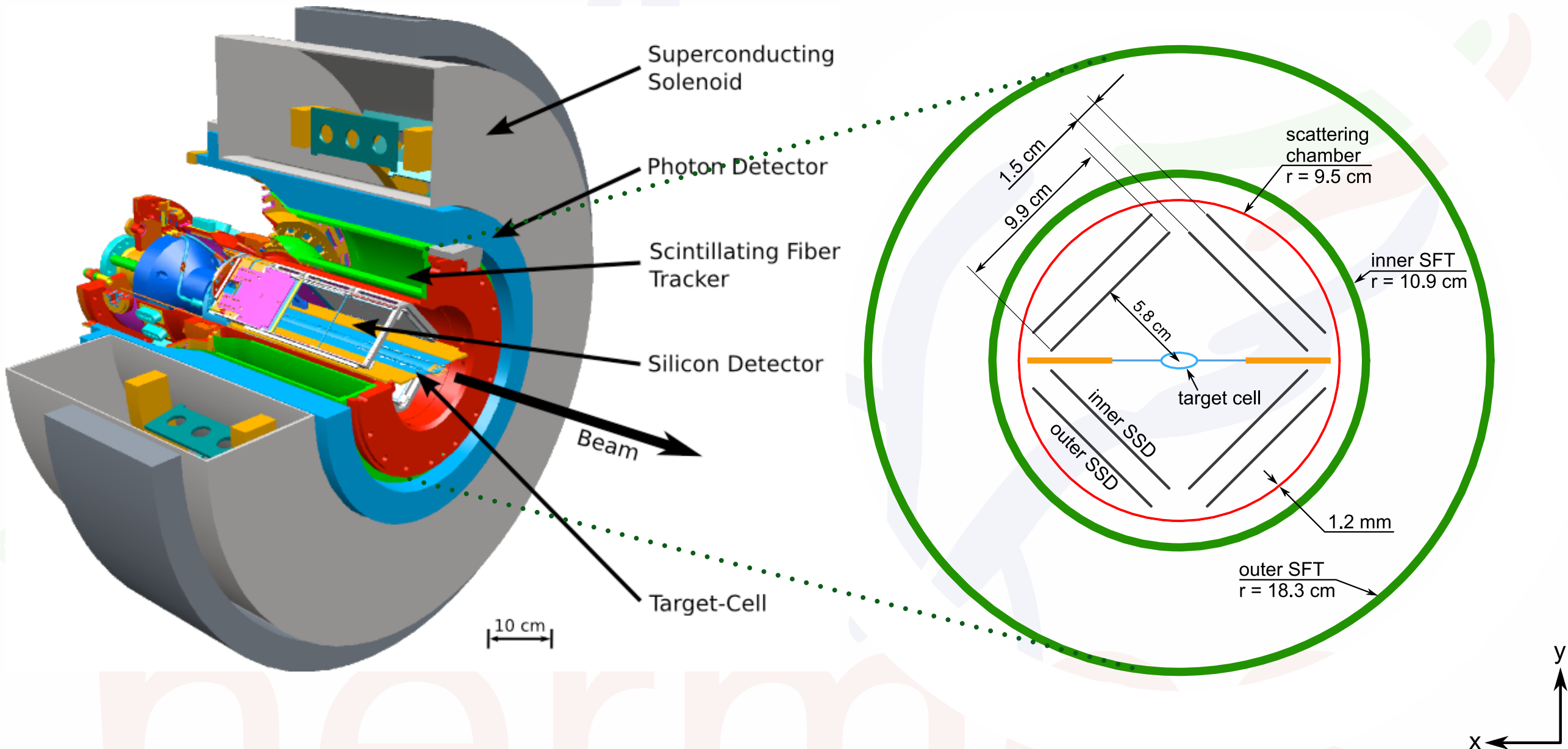
S

HERMES detector (2006/07)

detection of
recoiling proton



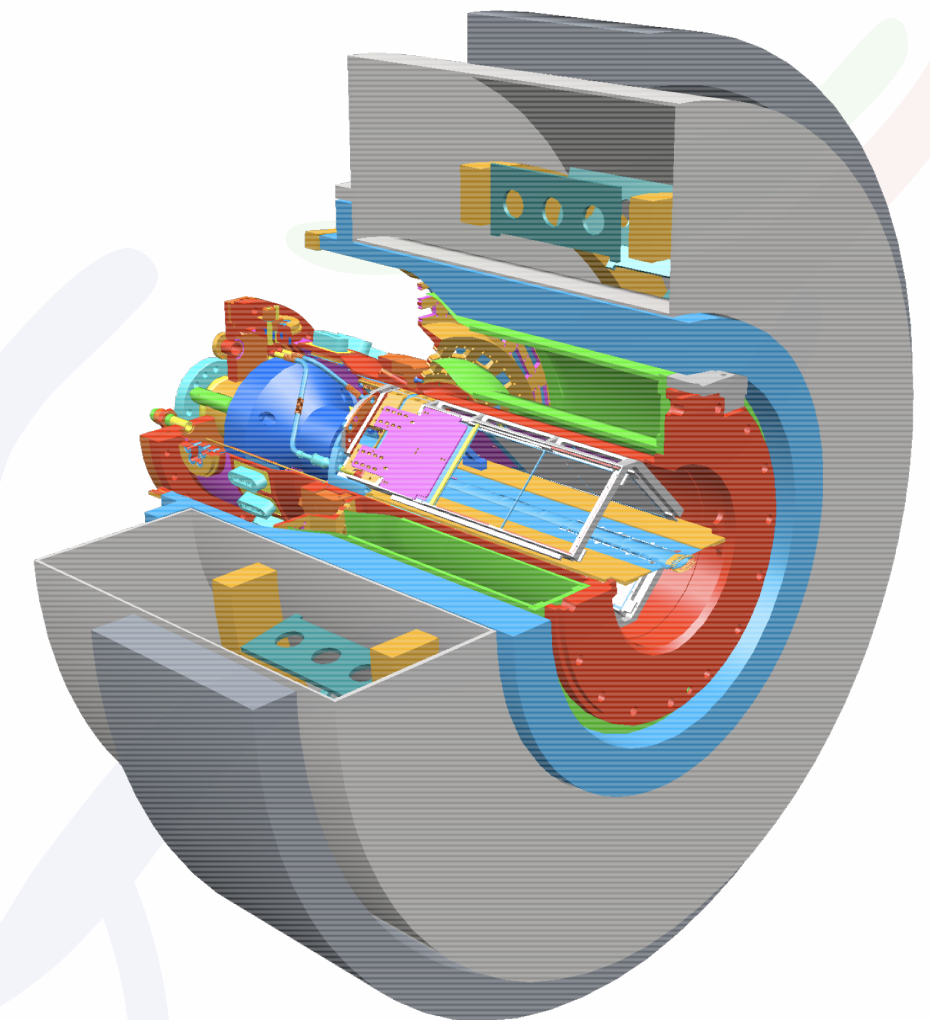
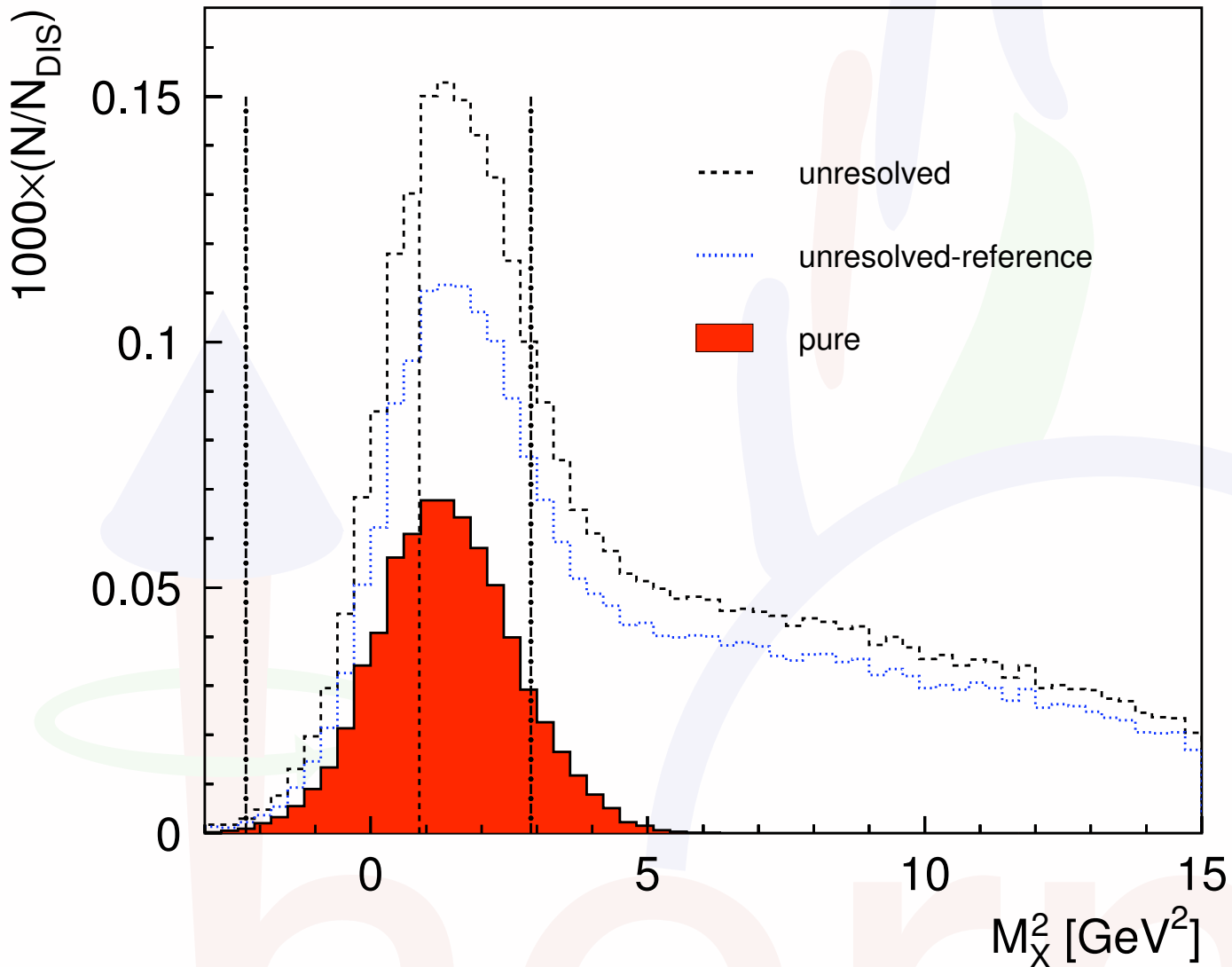
The HERMES Recoil detector



Enables the measurement of the recoiling charged particle and therefore full $e p \rightarrow e p \gamma$ event reconstruction

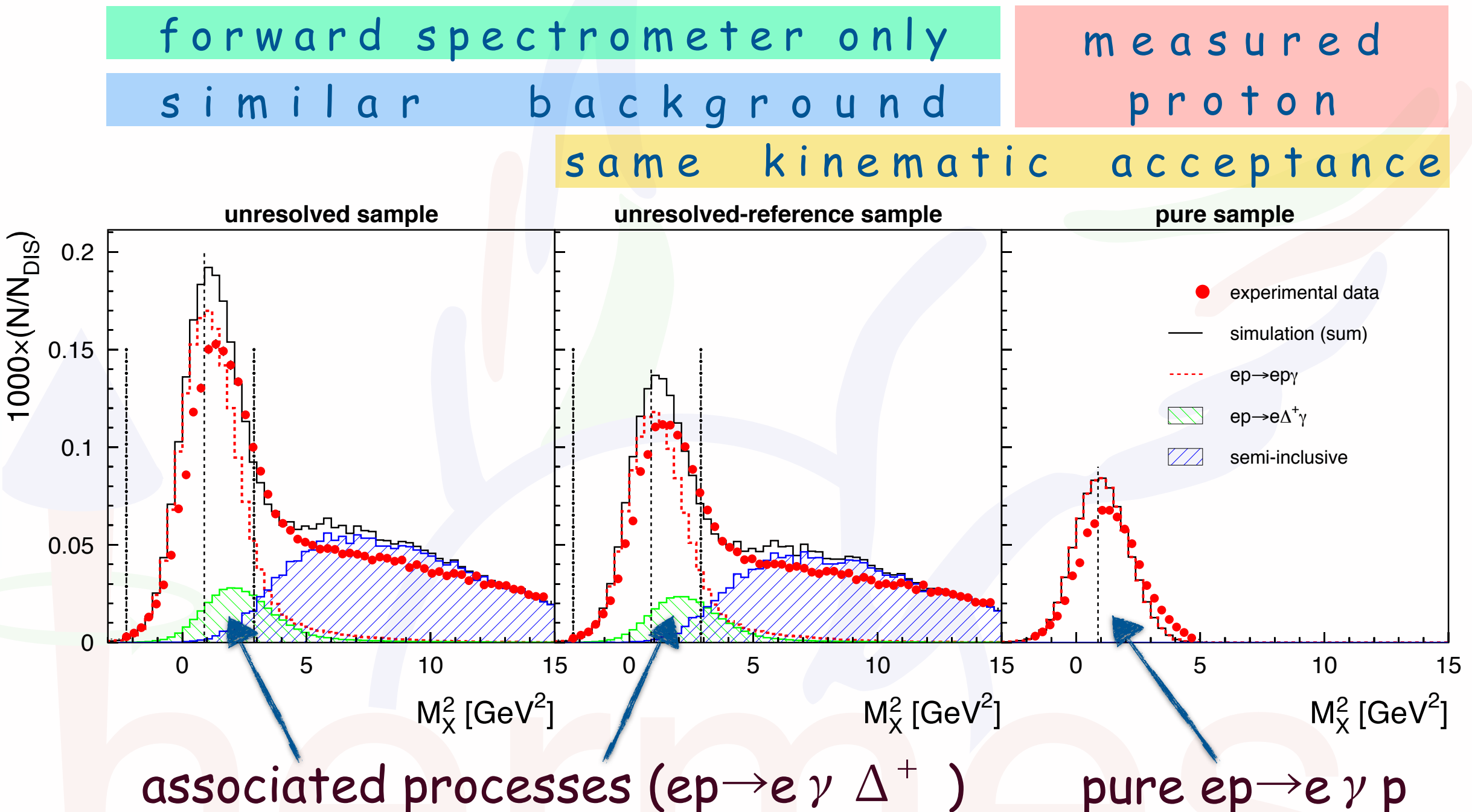
HERMES detector (2006/07)

kinematic fitting



- All particles in final state detected \rightarrow 4 constraints from energy-momentum conservation
- Selection of **pure BH/DVCS ($e p \rightarrow e p \gamma$)** with **high efficiency (~83%)**
- Allows to suppress background from associated and semi-inclusive processes to a negligible level (<0.2%)

Exclusivity with recoil detector

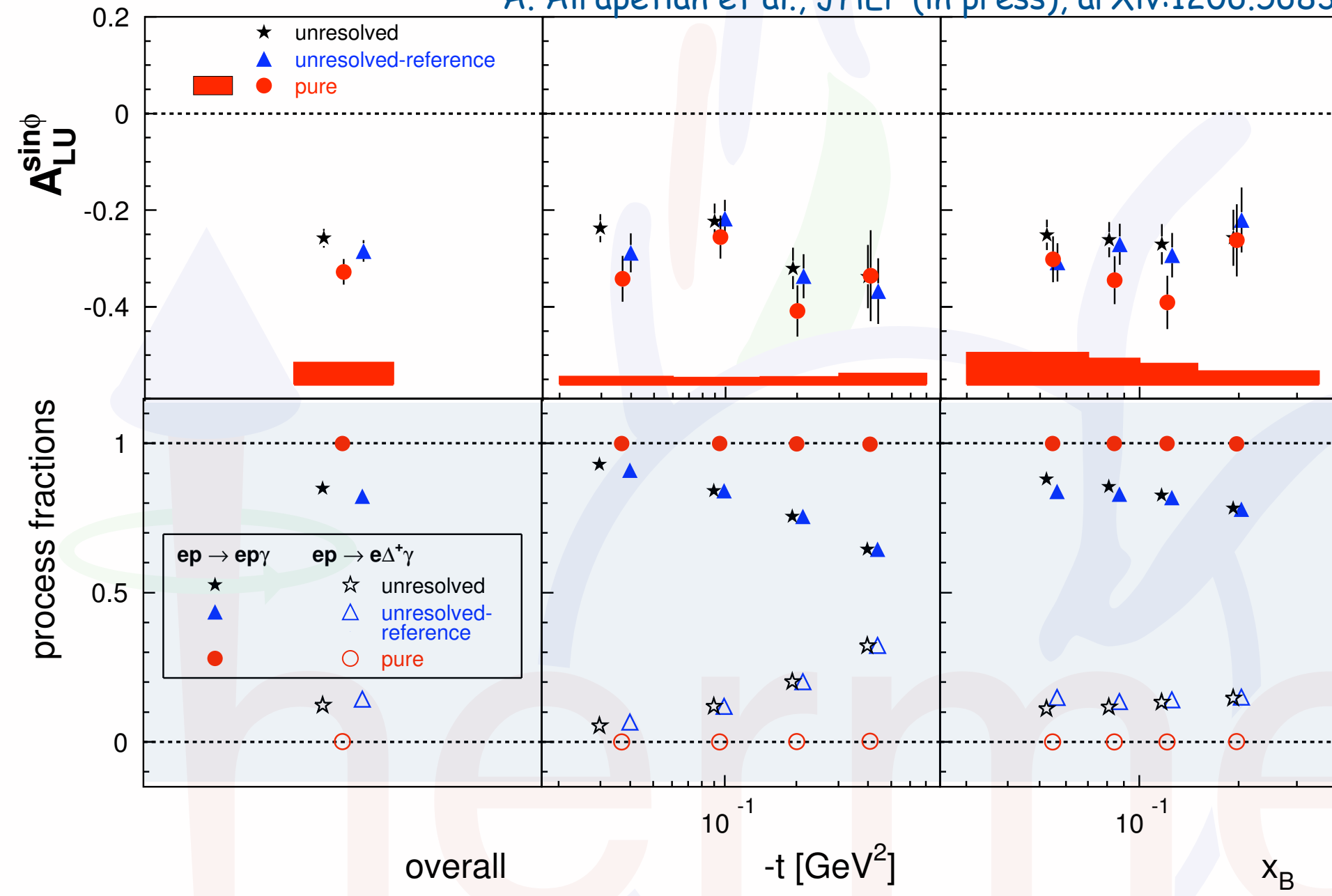


Missing mass:

$$M_x^2 = (k - k' + P_0 - P_\gamma)^2 = M^2 + 2M(\nu - E_\gamma) + t$$

Single-charge BSA with recoil proton

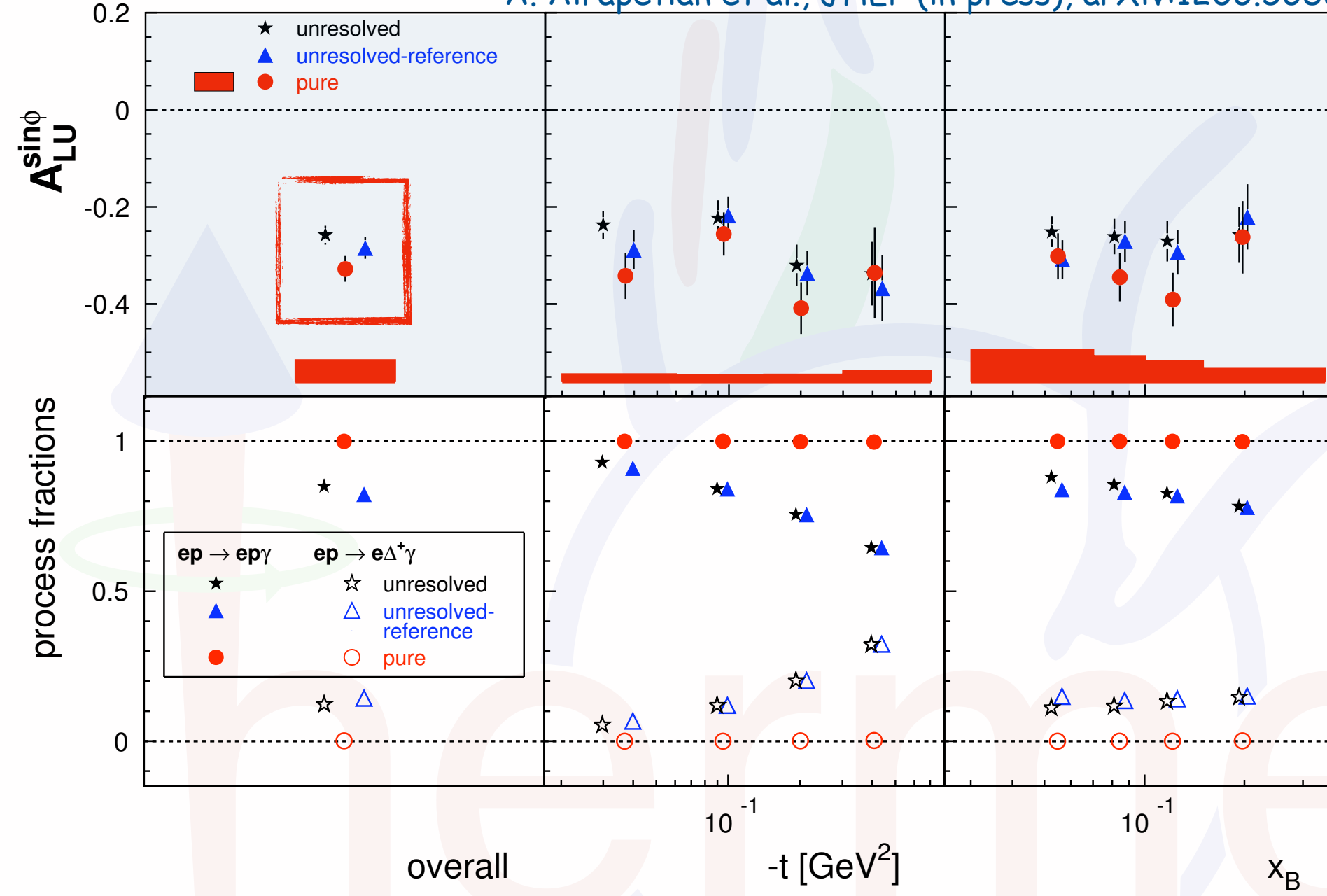
A. Airapetian et al., JHEP (in press), arXiv:1206.5683



basically no
contamination
→ clear interpretation

Single-charge BSA with recoil proton

A. Airapetian et al., JHEP (in press), arXiv:1206.5683

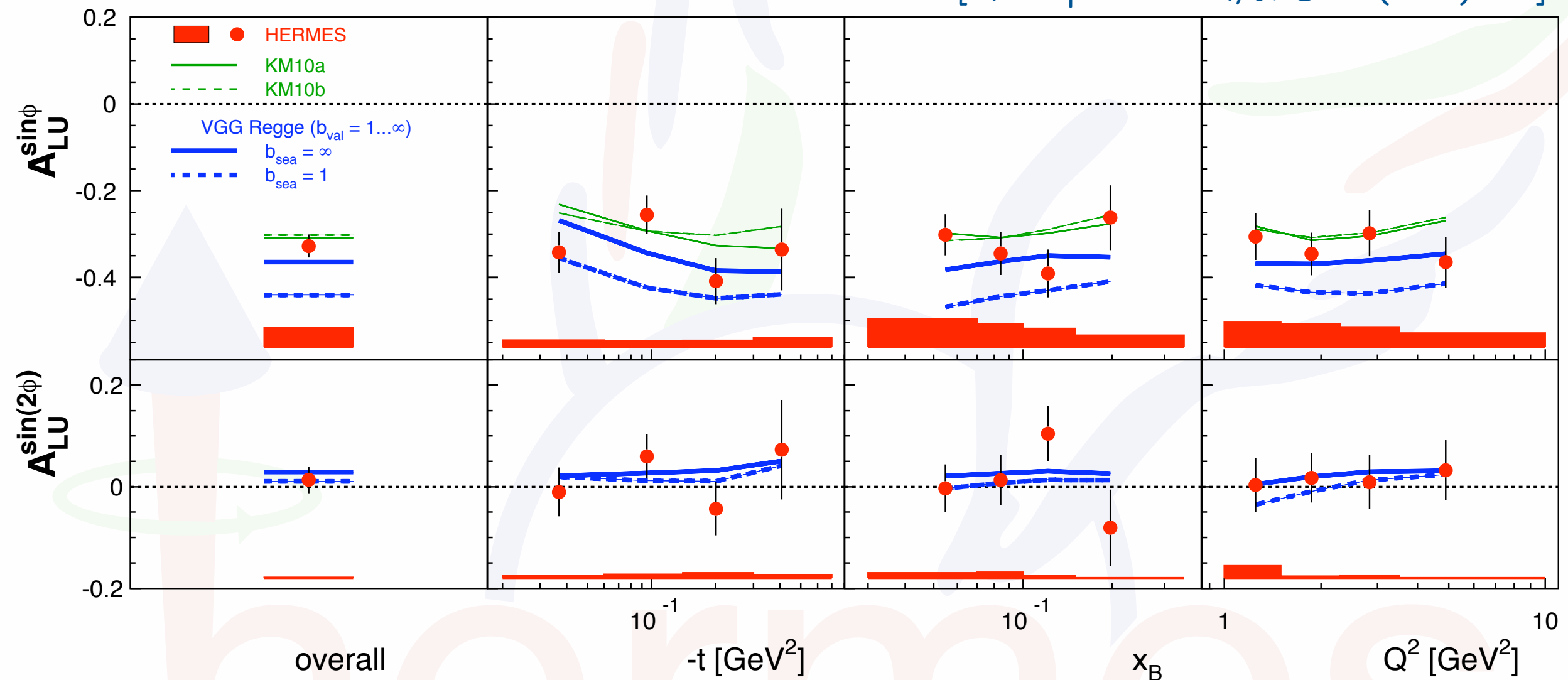


Magnitude of the leading asymmetry has increased by 0.054 ± 0.016
(\rightarrow assoc. in traditional analysis mainly dilution)

basically no contamination
 \rightarrow clear interpretation

Single-charge BSA with recoil proton

[A. Airapetian et al., JHEP 10 (2012) 042]

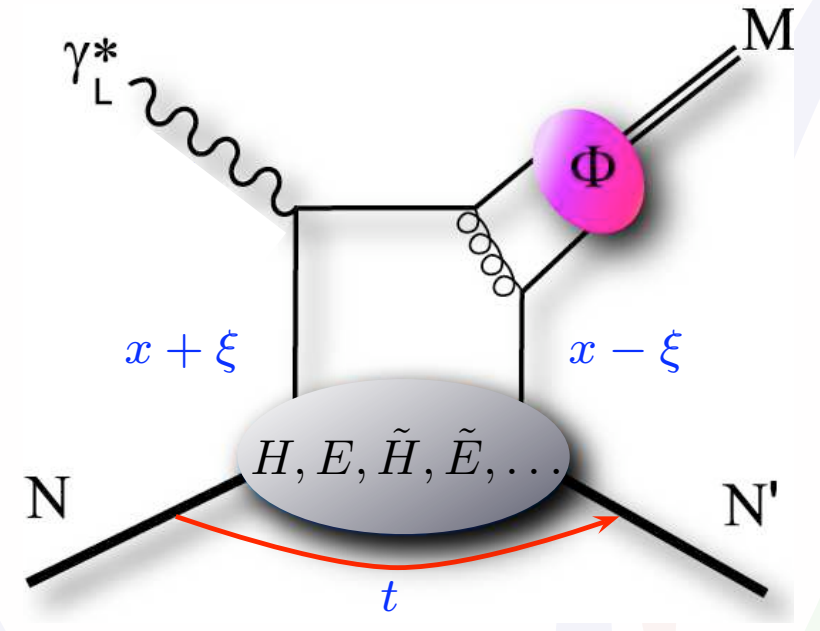


good agreement with models

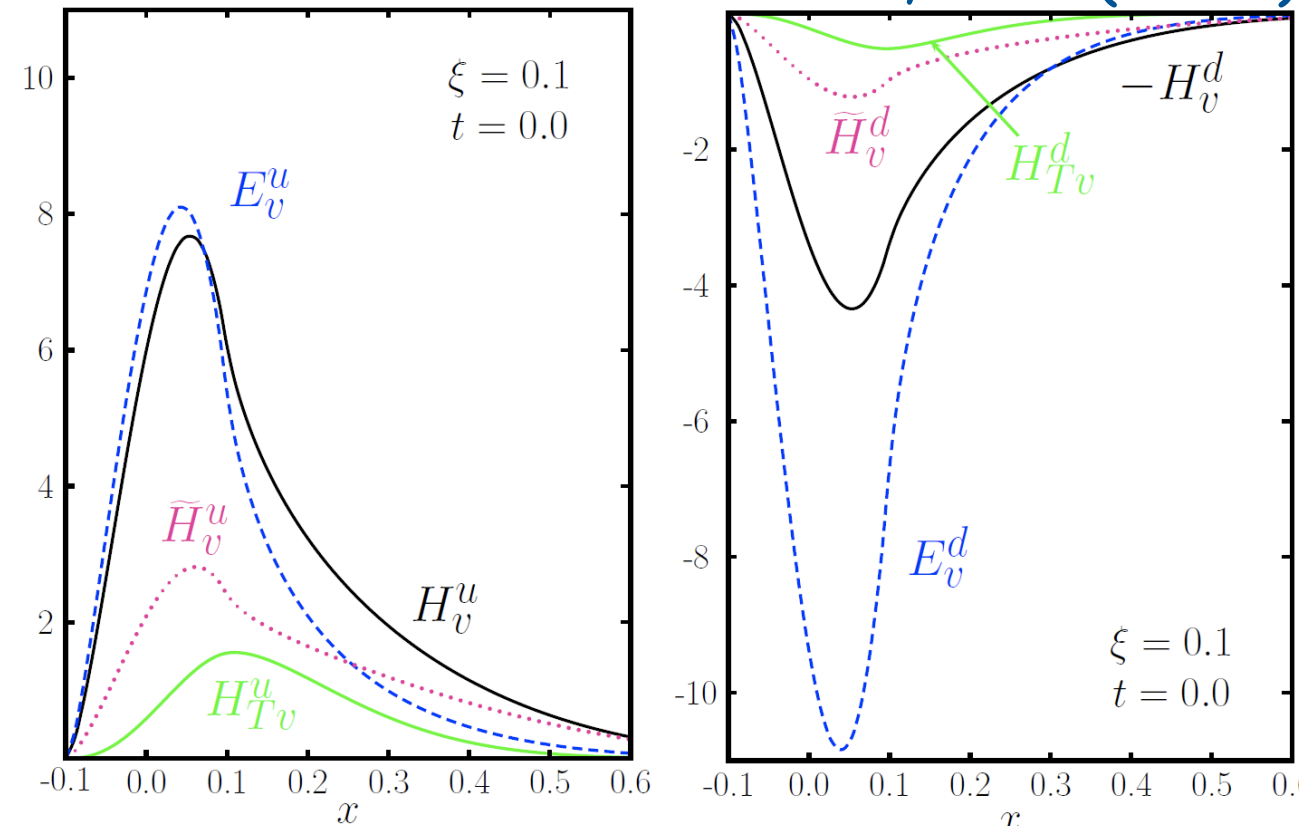
KM10 - K. Kumericki and D. Müller, Nucl. Phys. B 841 (2010) 1

VGG - M. Vanderhaeghen et al., Phys. Rev. D 60 (1999) 094017

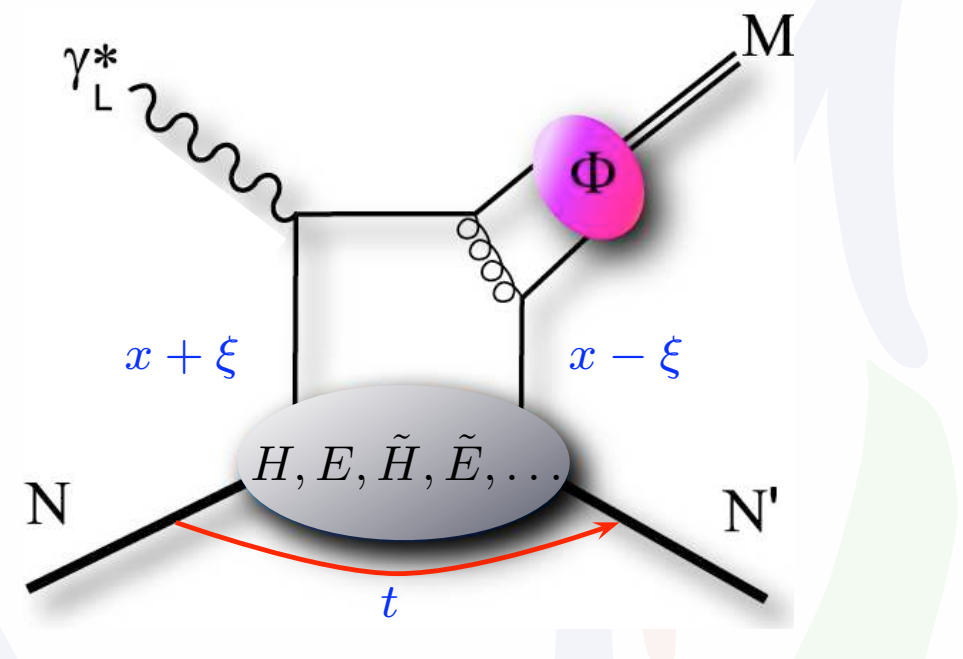
GPDs - a nice success story!



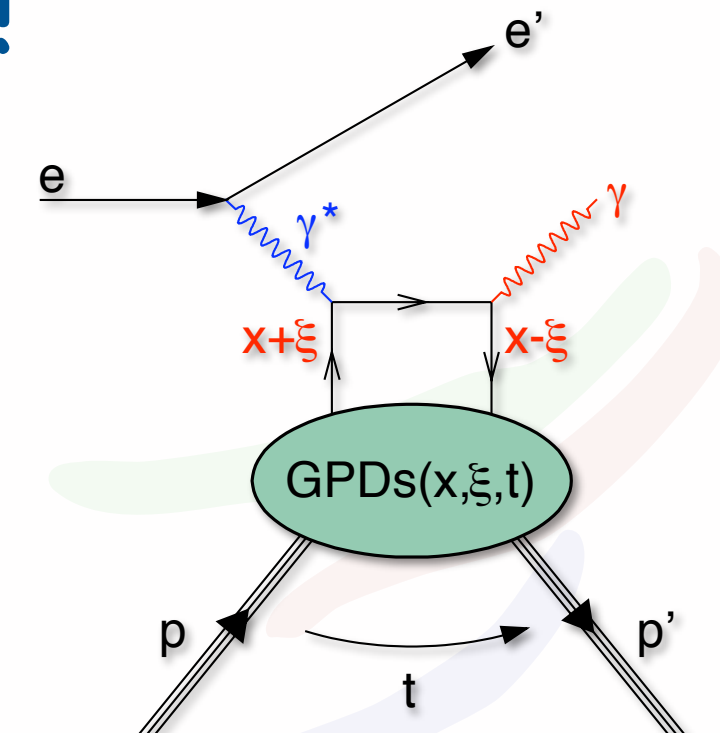
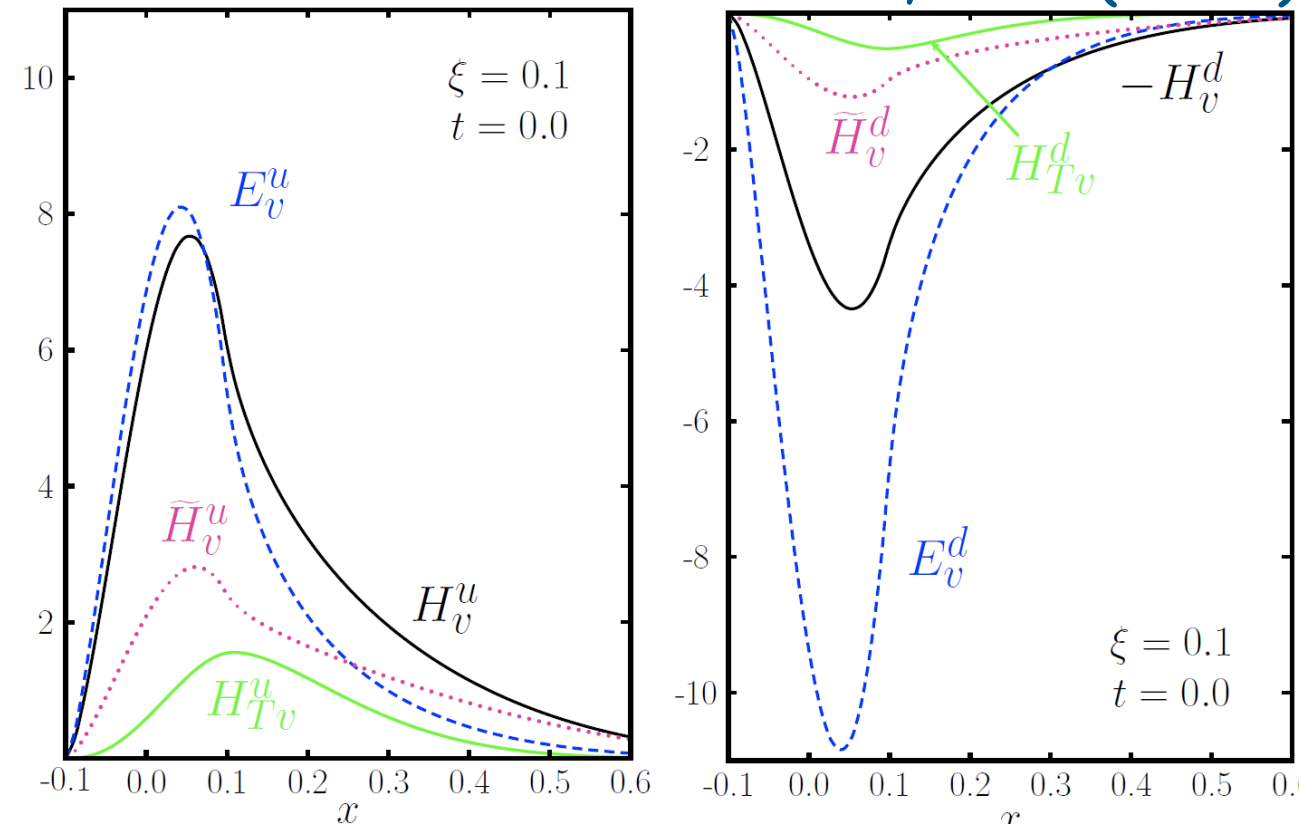
Goloskokov, Kroll (2007)



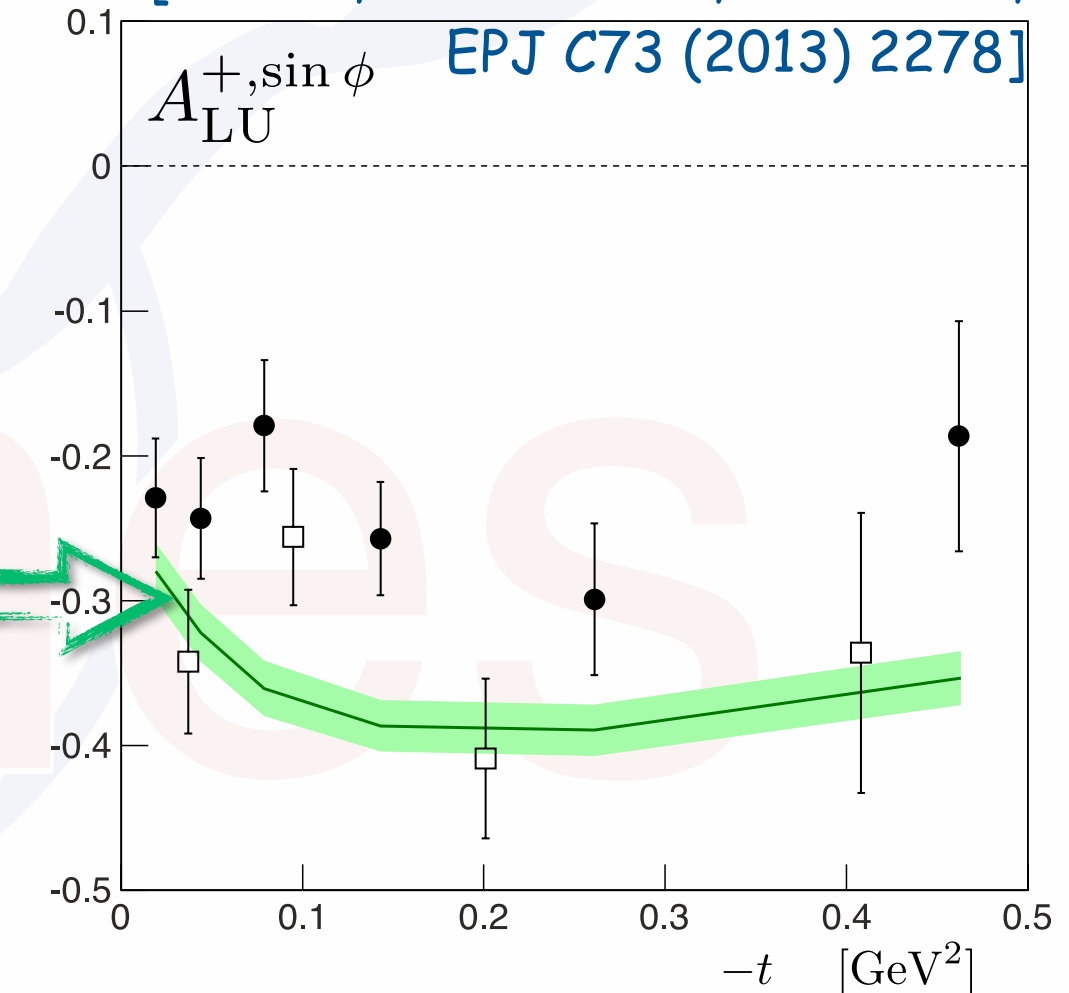
GPDs - a nice success story!



Goloskokov, Kroll (2007)

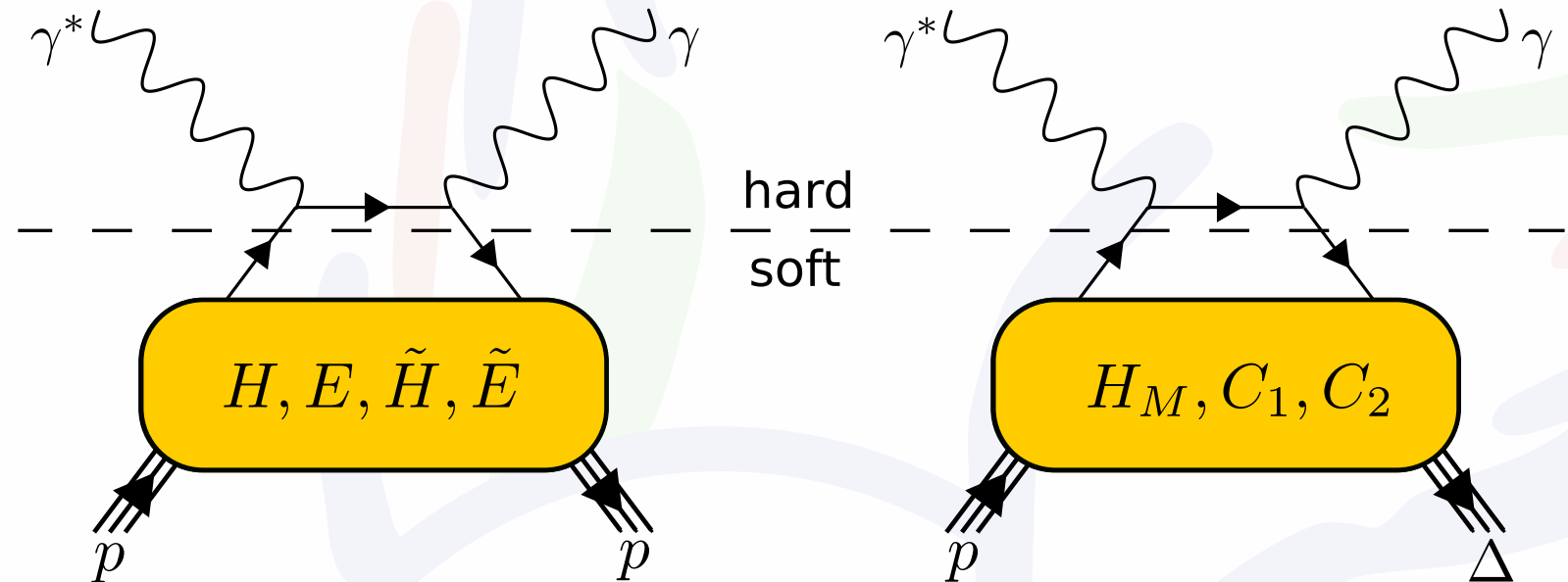


[P. Kroll, H. Moutarde, F. Sabatie,
EPJ C73 (2013) 2278]



Beam-spin asymmetries $e p \rightarrow e \gamma N \pi$

Besides a better understanding of the unresolved sample, associated DVCS in principle also allows further access to GPDs.

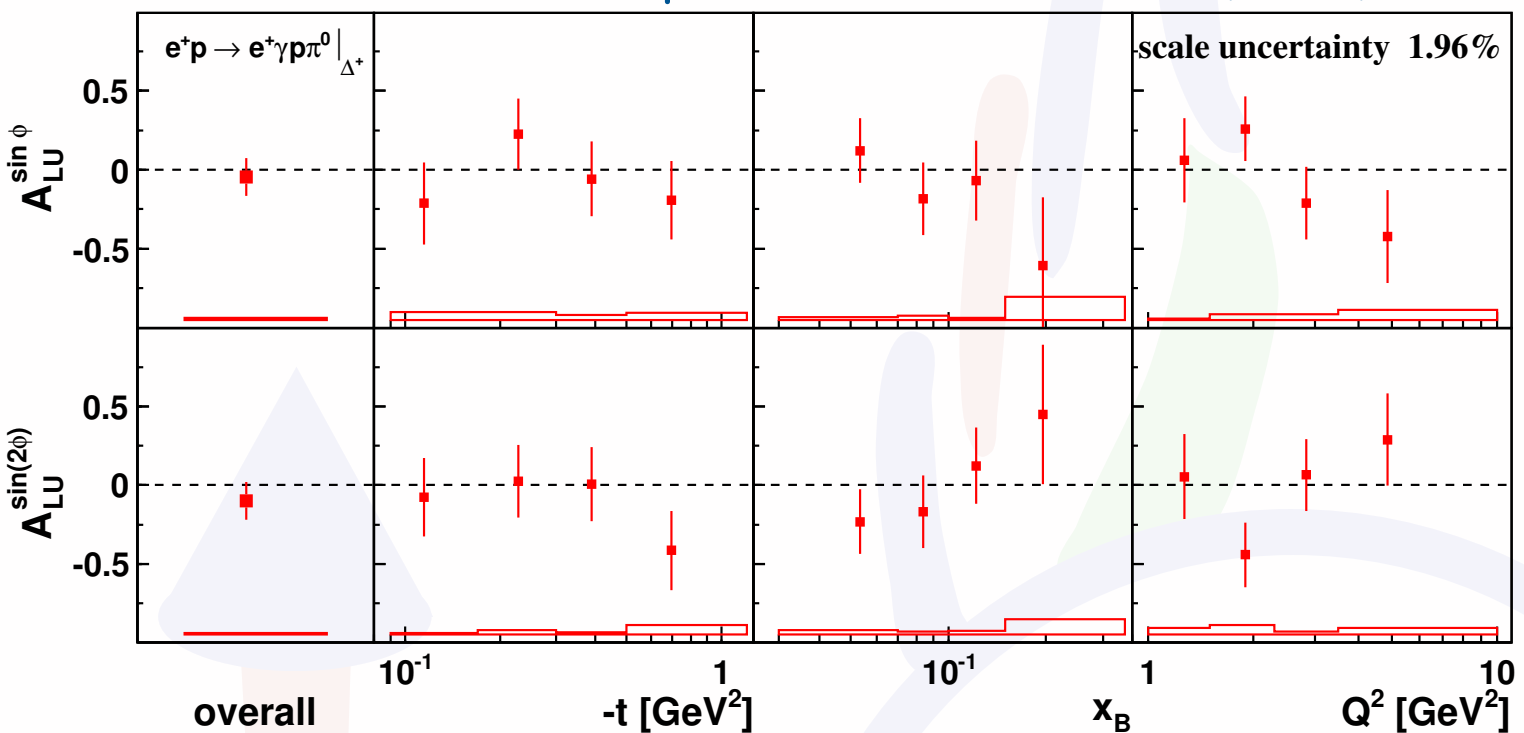


In the large- N_c limit the remaining $N \rightarrow \Delta$ GPDs can be related to the
N \rightarrow N iso-vector GPDs:

$$H_M(x, \xi, t) = \frac{2}{\sqrt{3}} [E^u(x, \xi, t) - E^d(x, \xi, t)],$$
$$C_1(x, \xi, t) = \sqrt{3} [\tilde{H}^u(x, \xi, t) - \tilde{H}^d(x, \xi, t)],$$
$$C_2(x, \xi, t) = \frac{\sqrt{3}}{4} [\tilde{E}^u(x, \xi, t) - \tilde{E}^d(x, \xi, t)]$$

Beam-spin asymmetries $e p \rightarrow e \gamma p \pi^0$

[A. Airapetian et al, JHEP 01 (2014) 077]

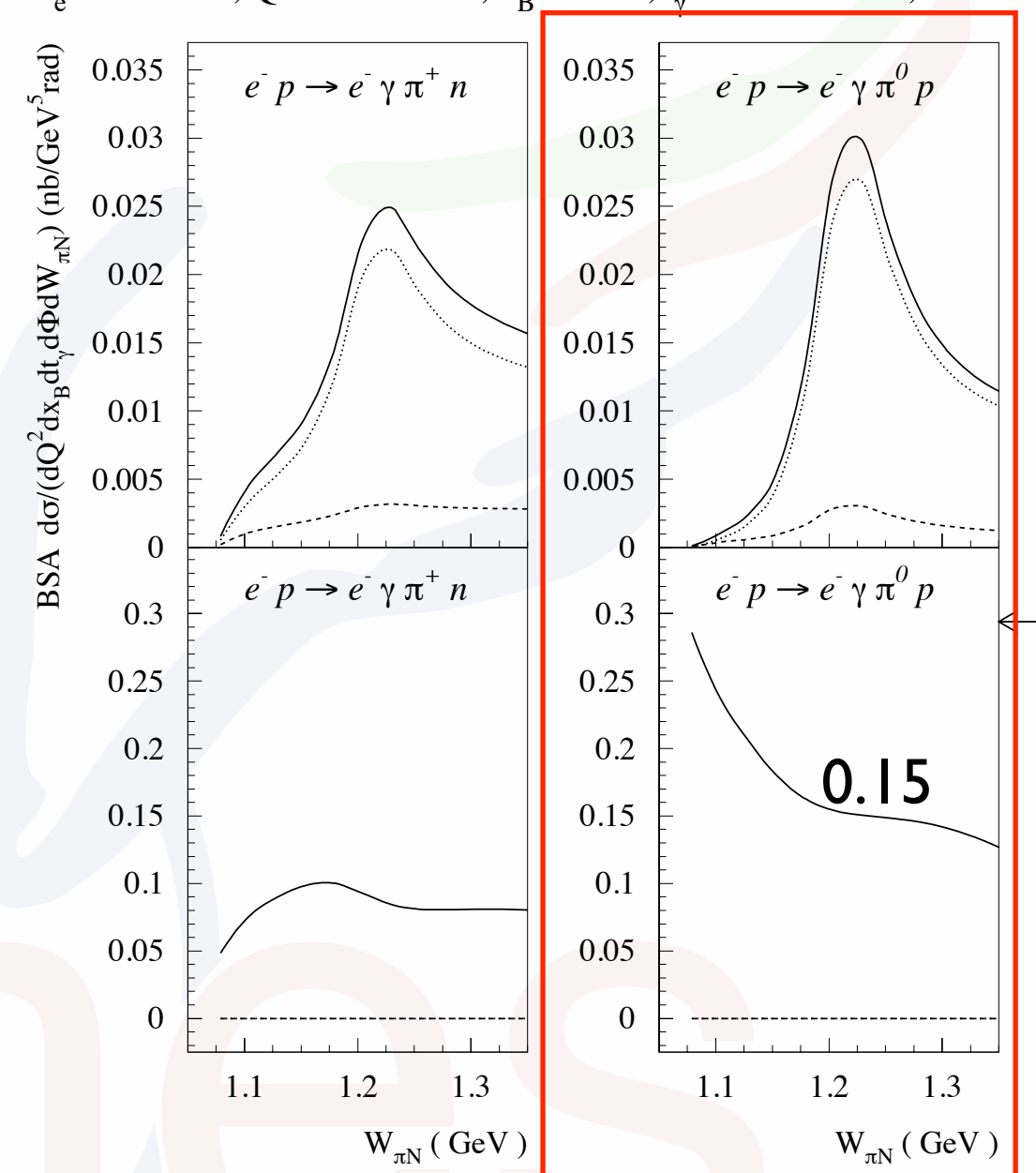


Shown amplitudes corrected for background
(only overall fractions are listed here):

Associated DVCS/BH ($e p \rightarrow e \gamma p \pi^0$)	85 ± 1
Elastic DVCS/BH ($e p \rightarrow e \gamma p$)	4.6 ± 0.1
SIDIS ($e p \rightarrow e X \pi^0$)	11 ± 1

[Guichon et al., PRD 68 (2003) 034018]

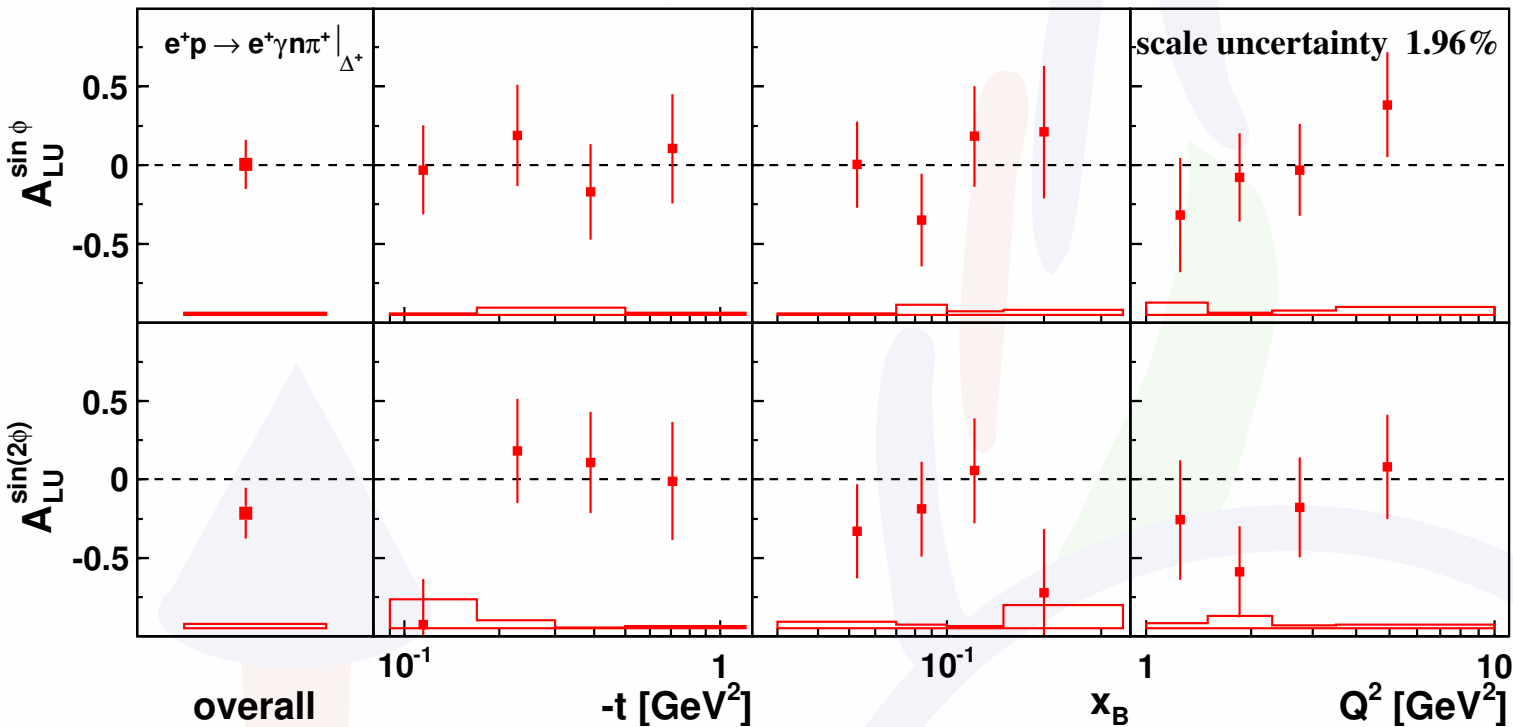
$E_e = 27 \text{ GeV}, Q^2 = 2.5 \text{ GeV}^2, x_B = 0.15, t_\gamma = -0.25 \text{ GeV}^2, \Phi = 90^\circ$



opposite sign convention!

Beam-spin asymmetries $e p \rightarrow e \gamma n \pi^+$

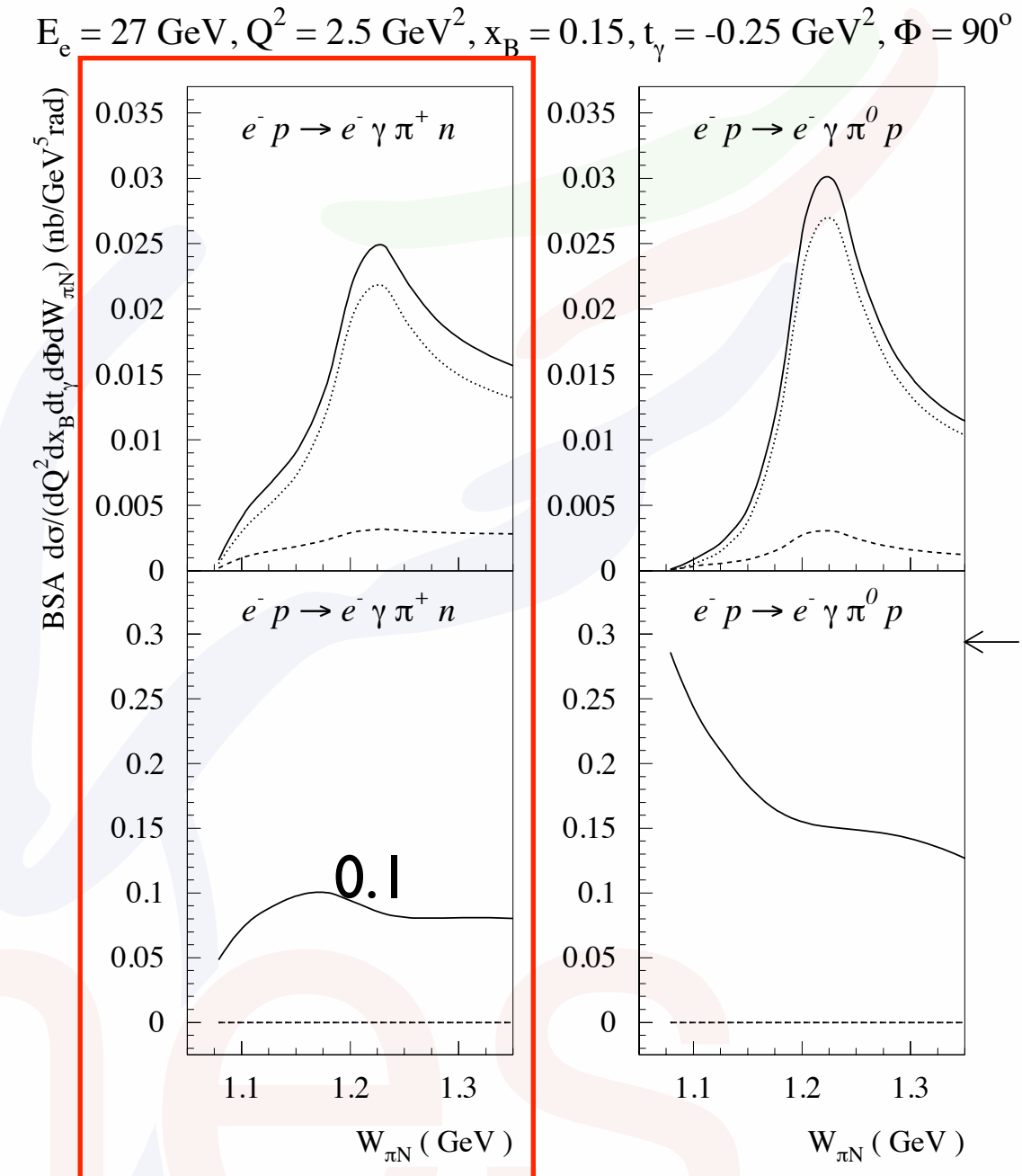
[A. Airapetian et al, JHEP 01 (2014) 077]



Shown amplitudes corrected for background
(only overall fractions are listed here):

Associated DVCS/BH ($e p \rightarrow e \gamma n \pi^+$)	77 ± 2
Elastic DVCS/BH ($e p \rightarrow e \gamma p$)	0.2 ± 0.1
SIDIS ($e p \rightarrow e X \pi^0$)	23 ± 3

[Guichon et al., PRD 68 (2003) 034018]



opposite sign convention!

DVCS at HERMES

HERMES analyzed a wealth of DVCS-related asymmetries on nucleon and nuclear targets

data with recoil-proton detection allows clean interpretation

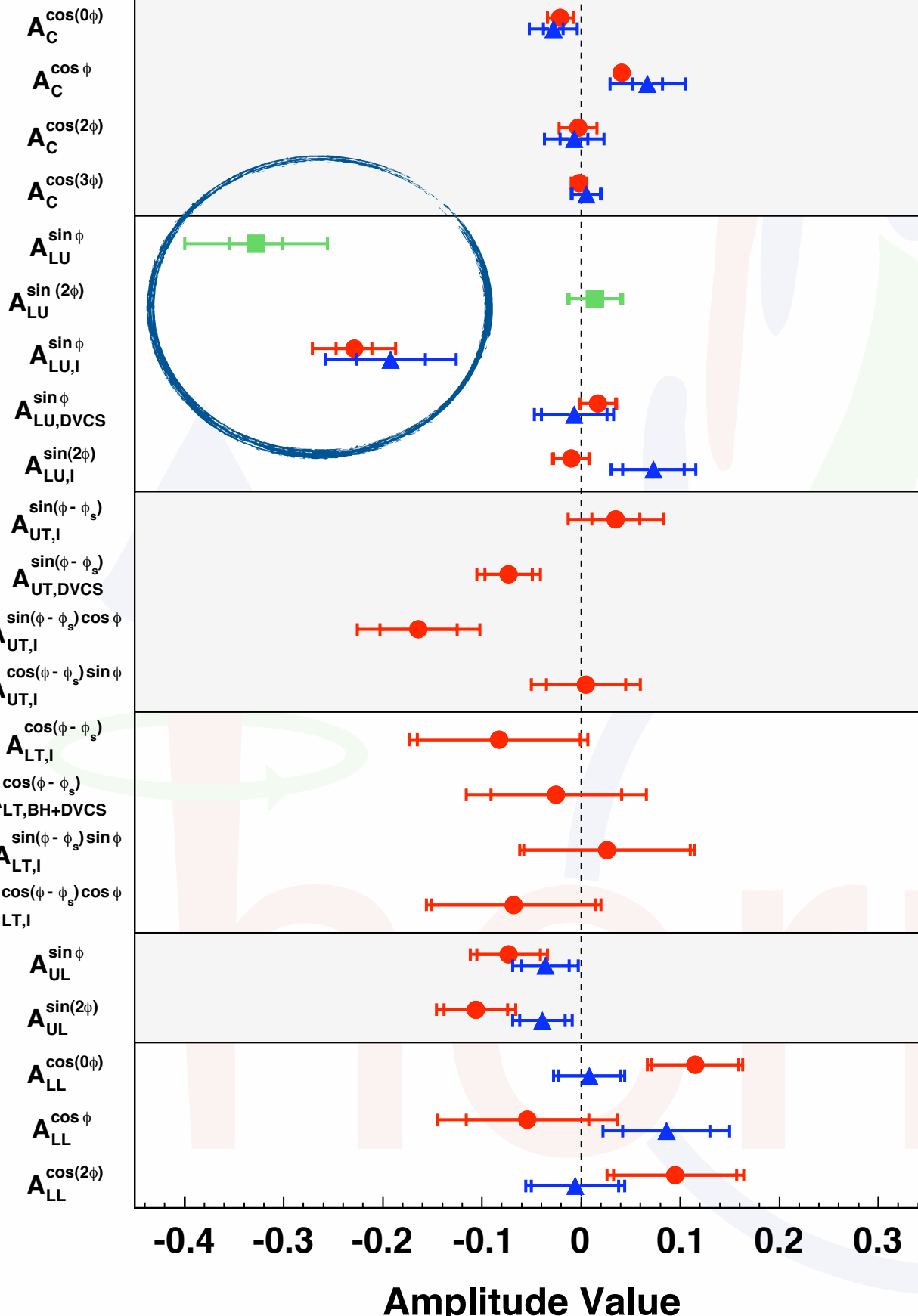
indication of larger amplitudes for pure sample

-> assoc. DVCS in "traditional" analysis mainly dilution, supported by recent results from HERMES
[JHEP 01 (2014) 077]:

assoc. DVCS results consistent with zero but also with model prediction

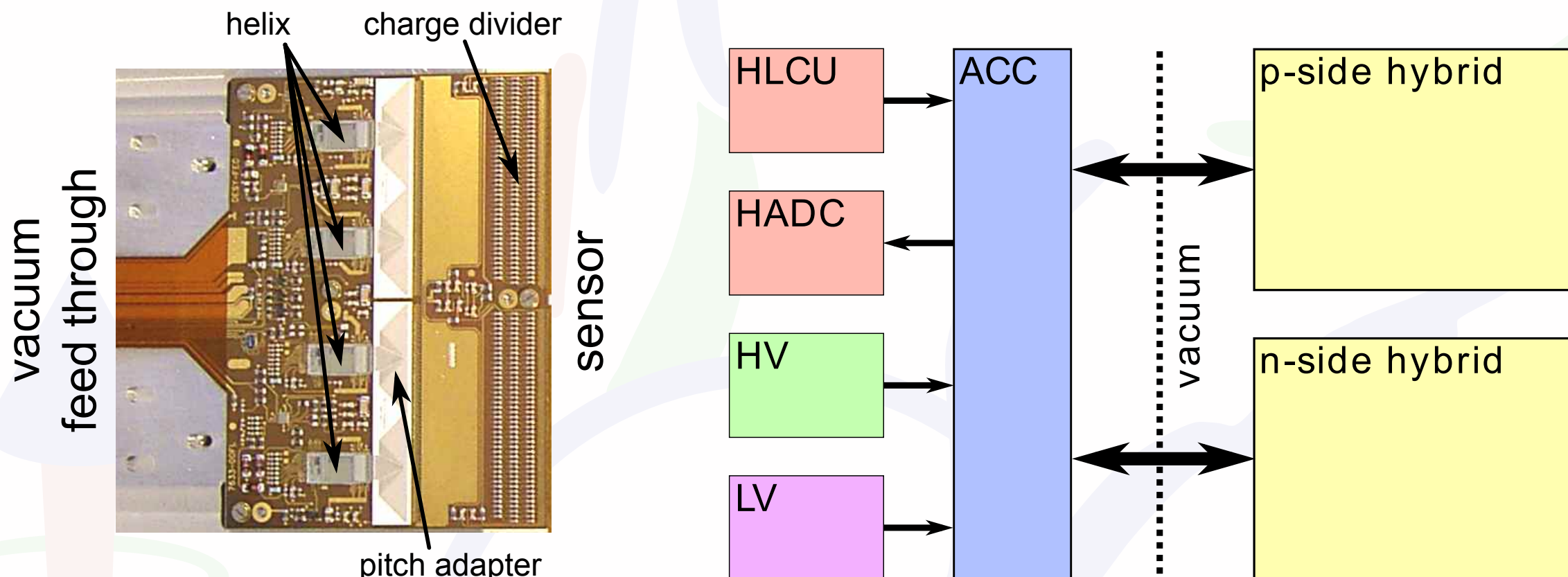
HERMES DVCS

- Hydrogen
- ▲ Deuterium
- Hydrogen Pure



Backup

SSD (silicon strip detector)



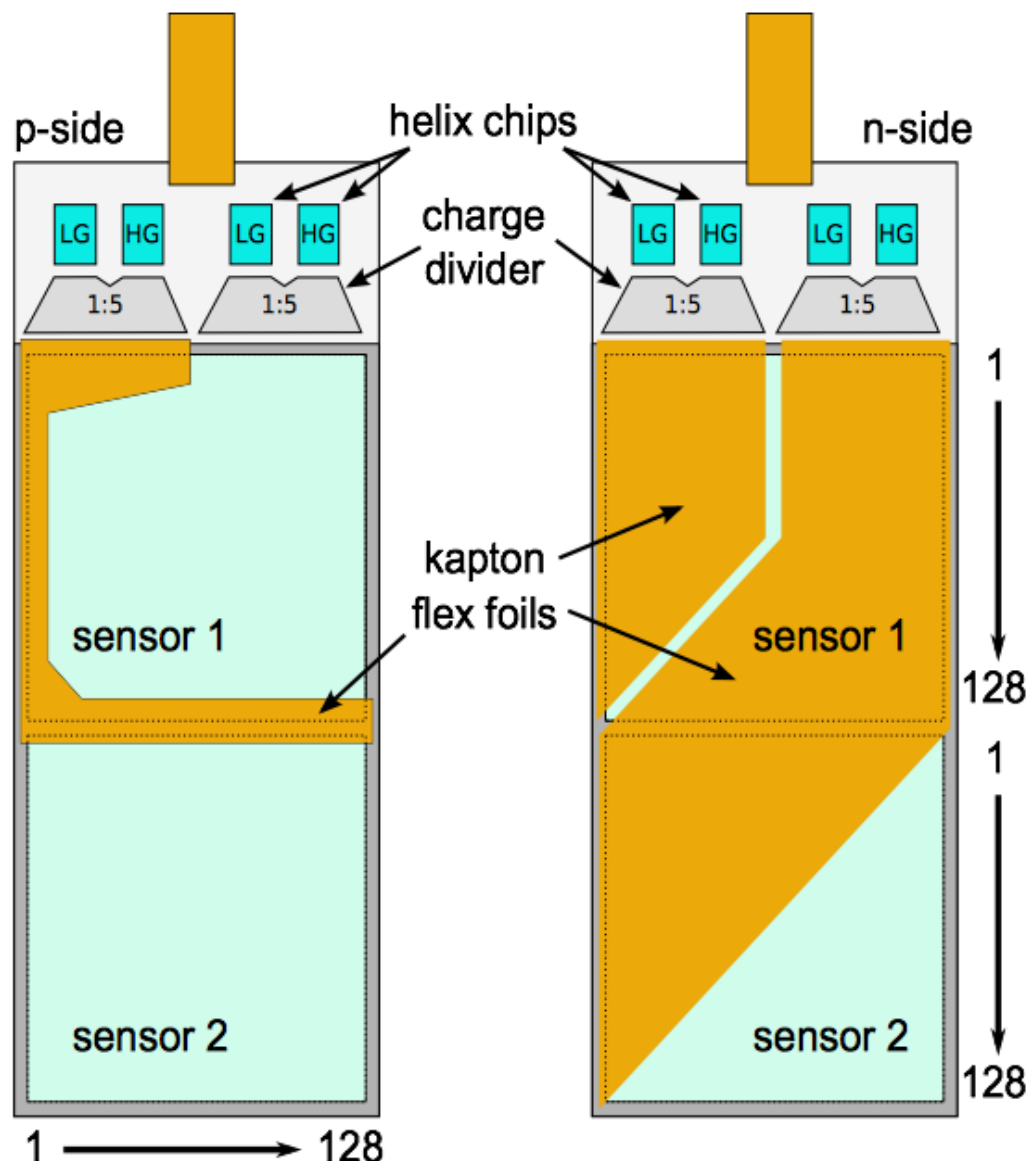
5.8 cm away from lepton beam, 1.5 cm gap

sensor thickness $295 \mu\text{m} - 315 \mu\text{m}$

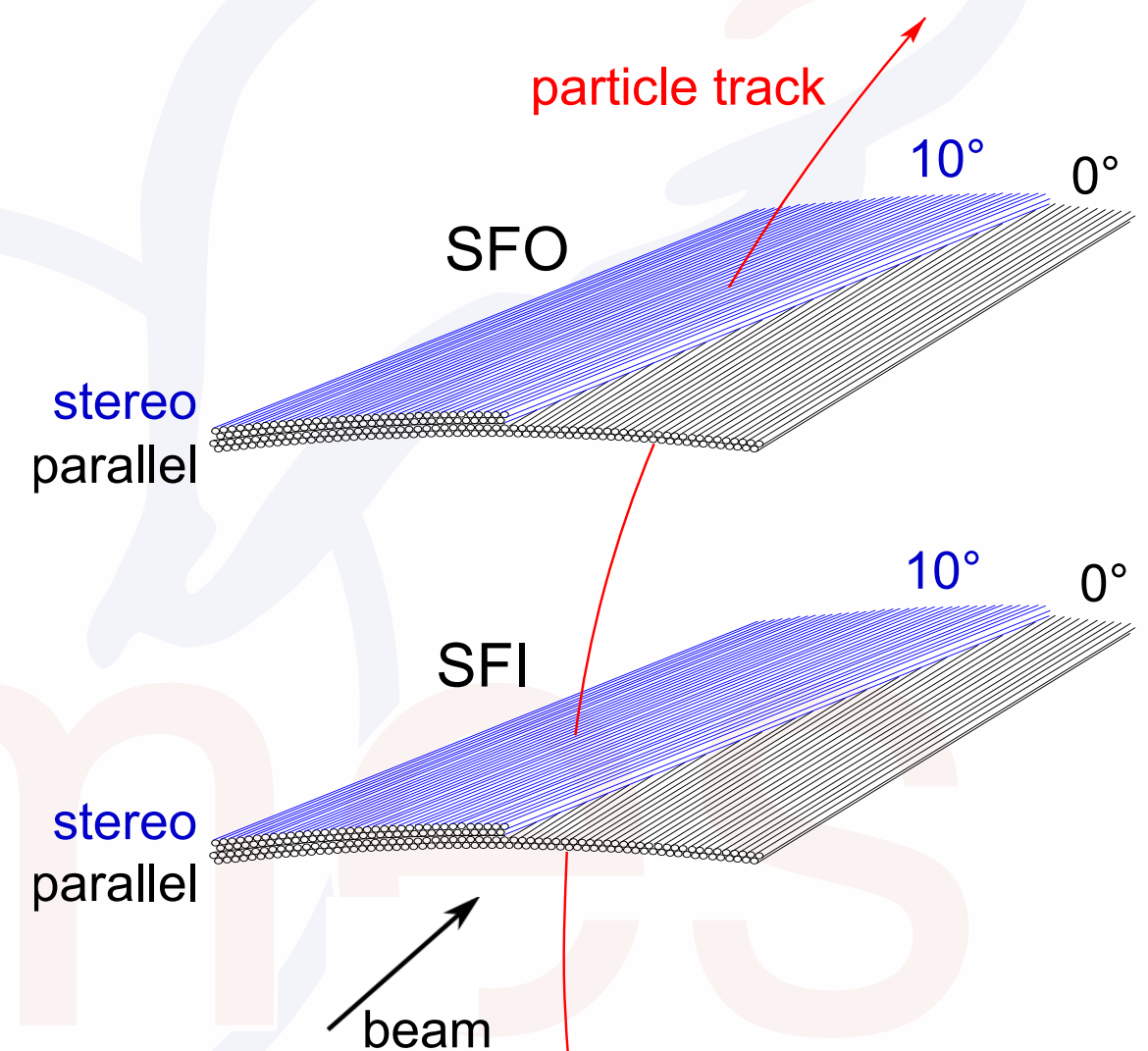
thickness of target cell $75 \mu\text{m}$

The HERMES recoil detector

Sketch of front- and backside of a silicon strip detector module (SSD)

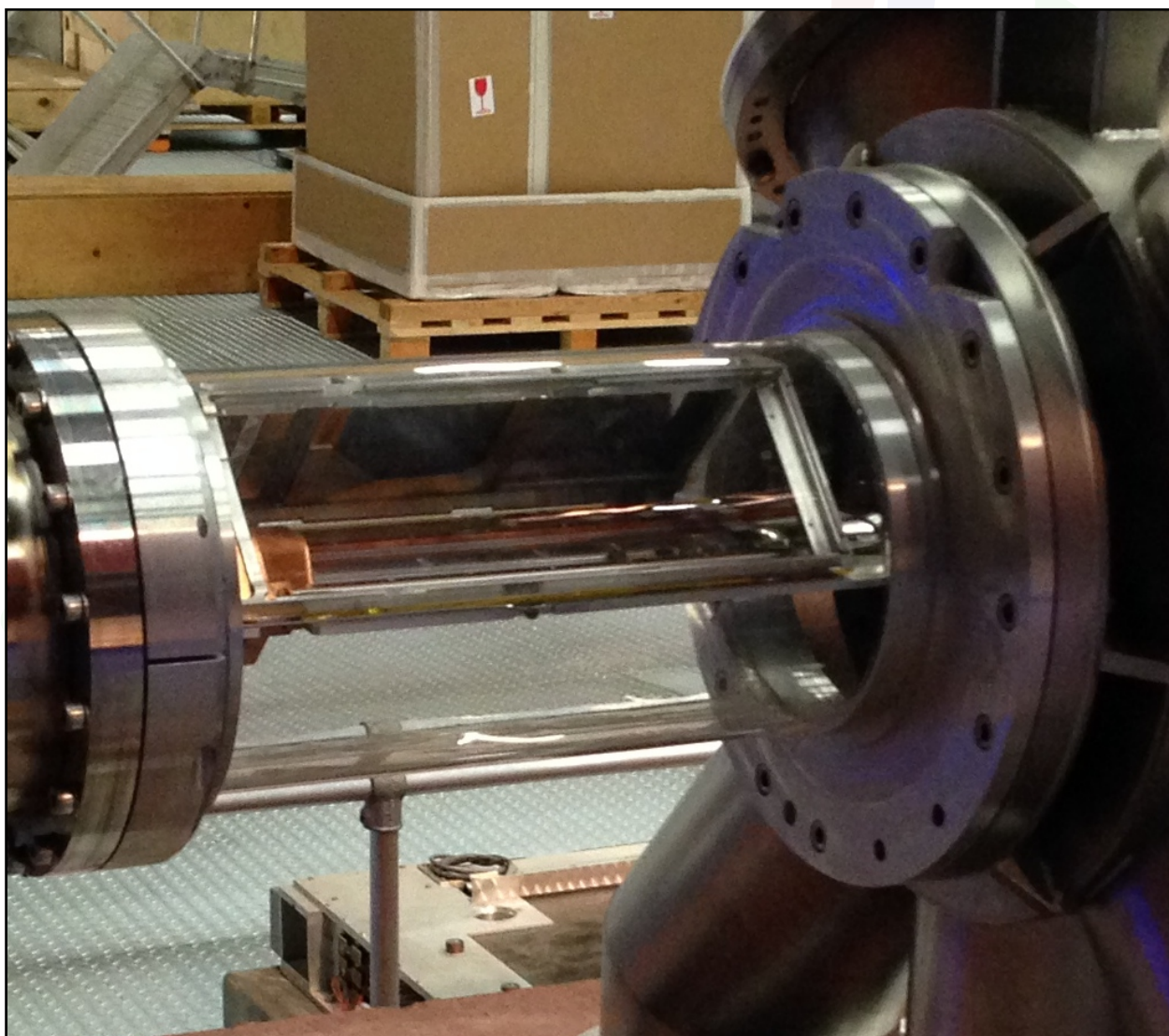


Schematic design of the scintillating fibre tracker (SFT)

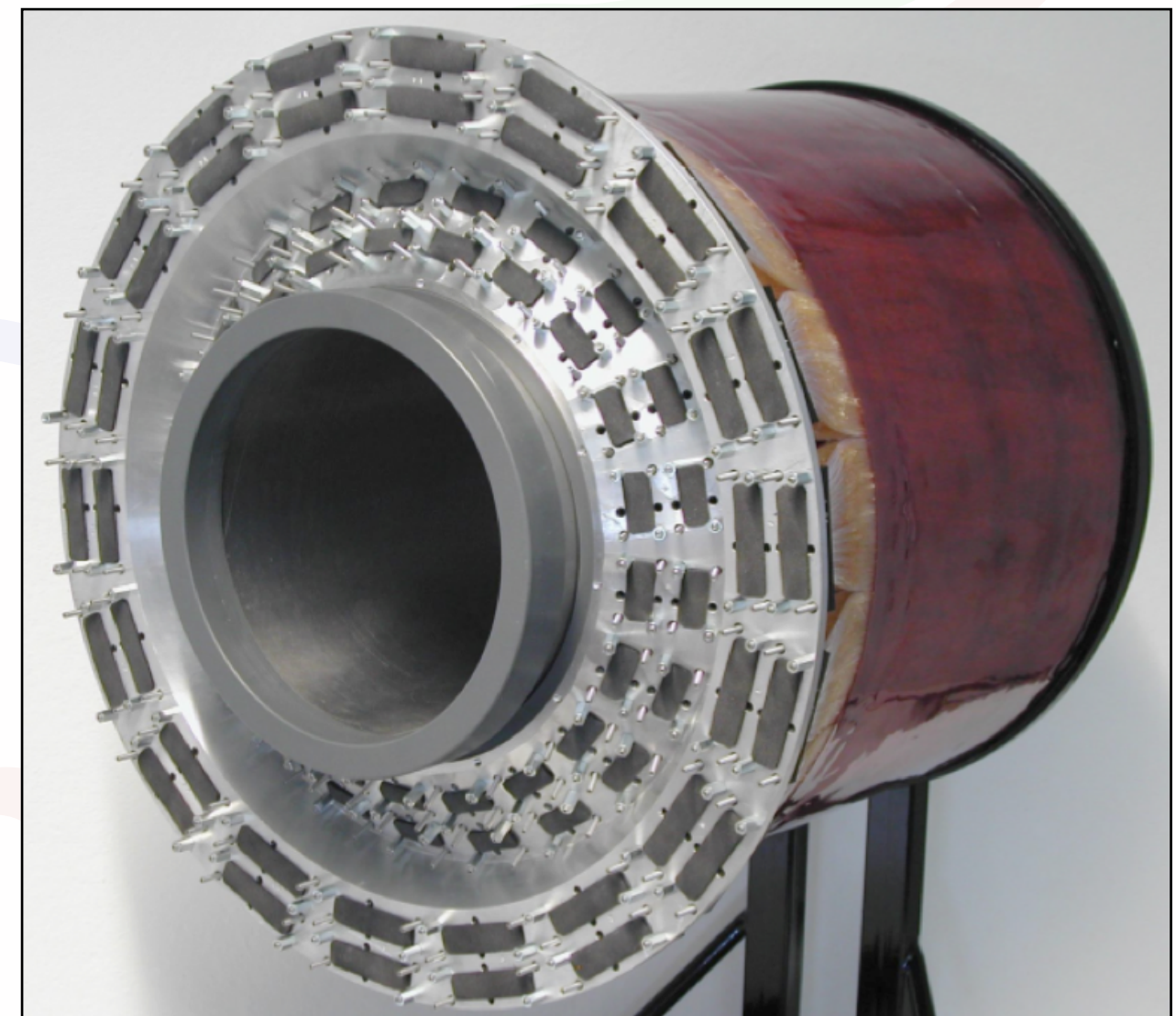


The HERMES recoil detector

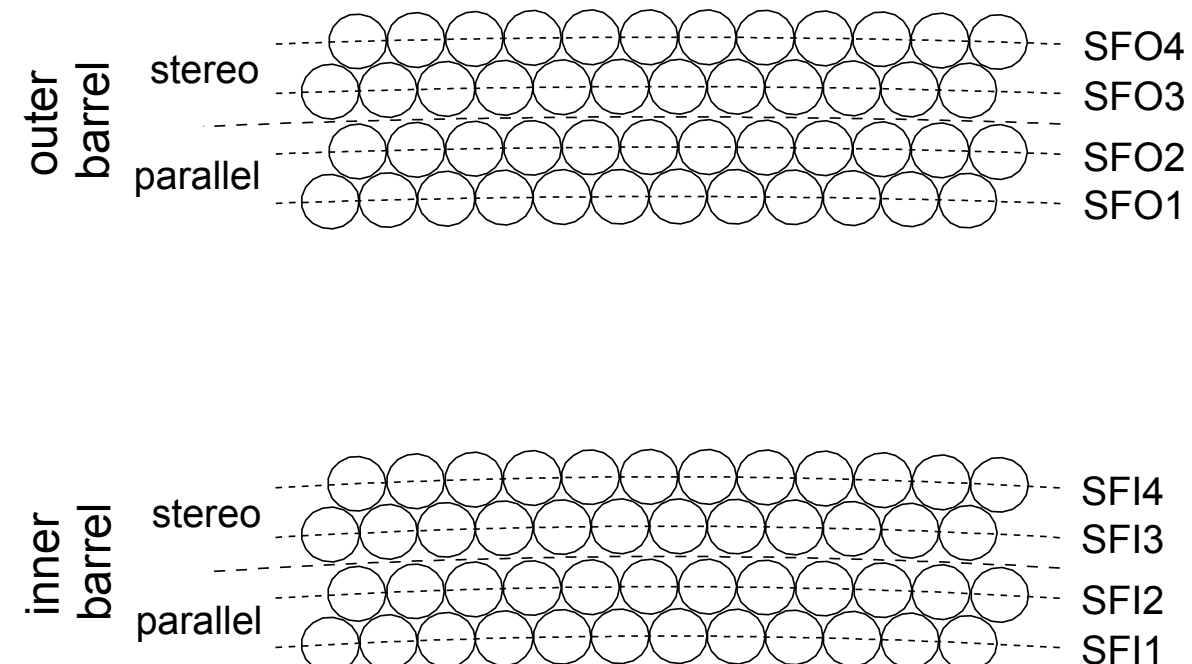
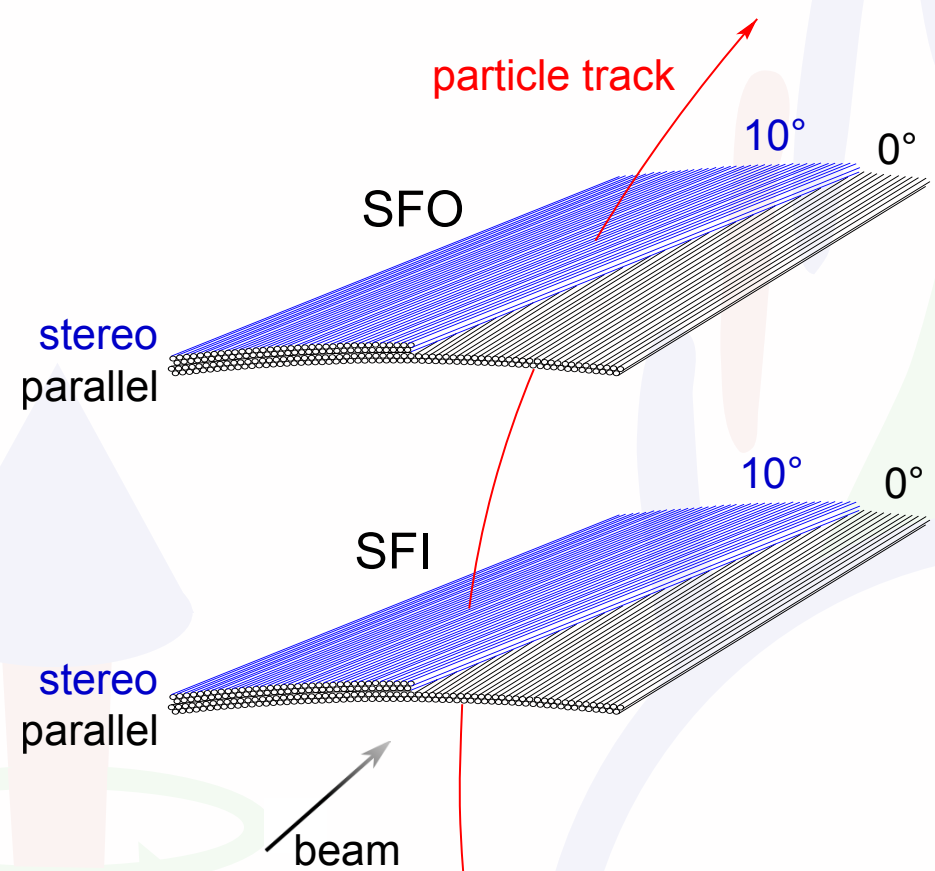
The silicon strip detector (SSD)



The scintillating fibre tracker (SFT)



SFT (scintillating fibre tracker)

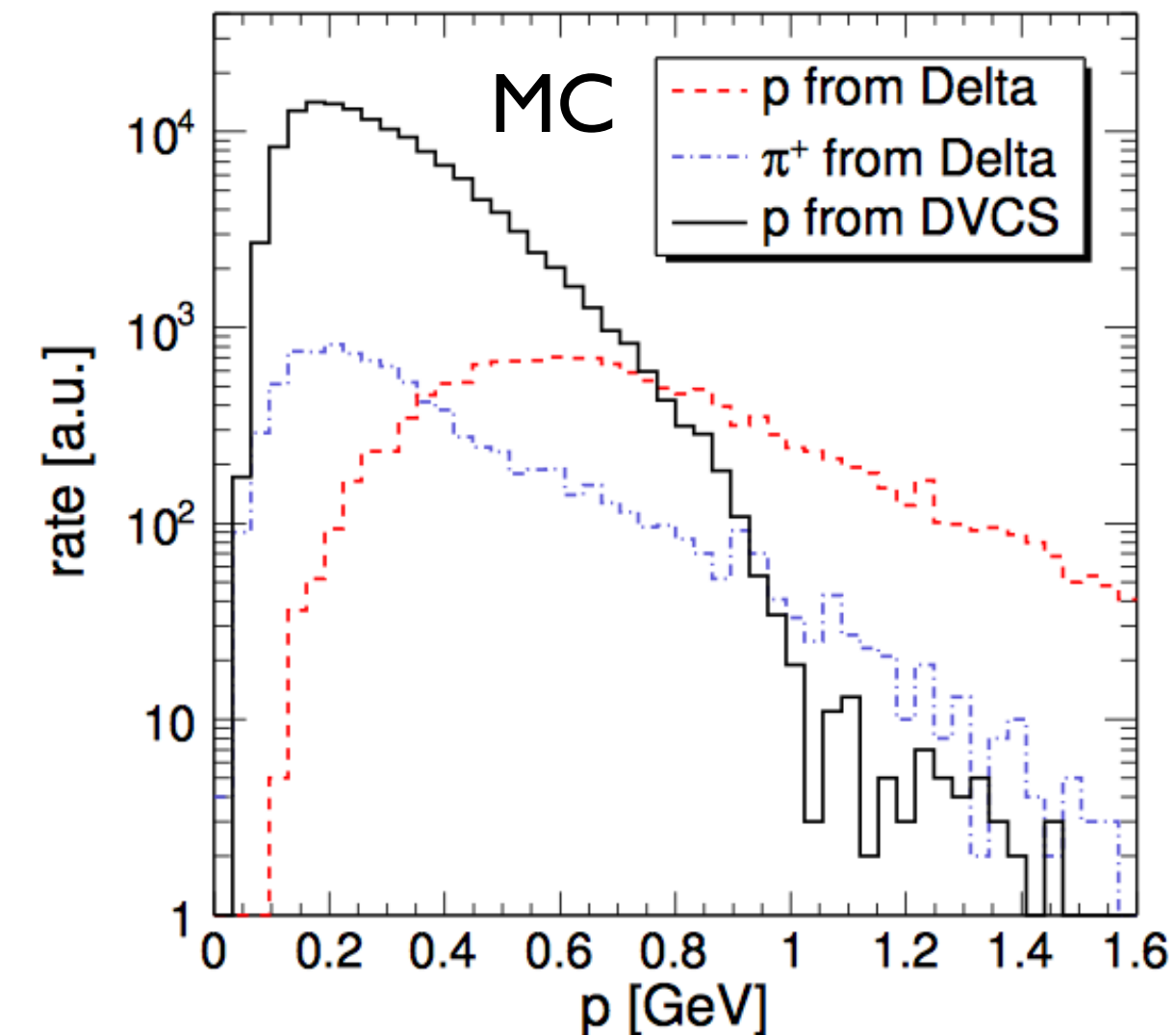
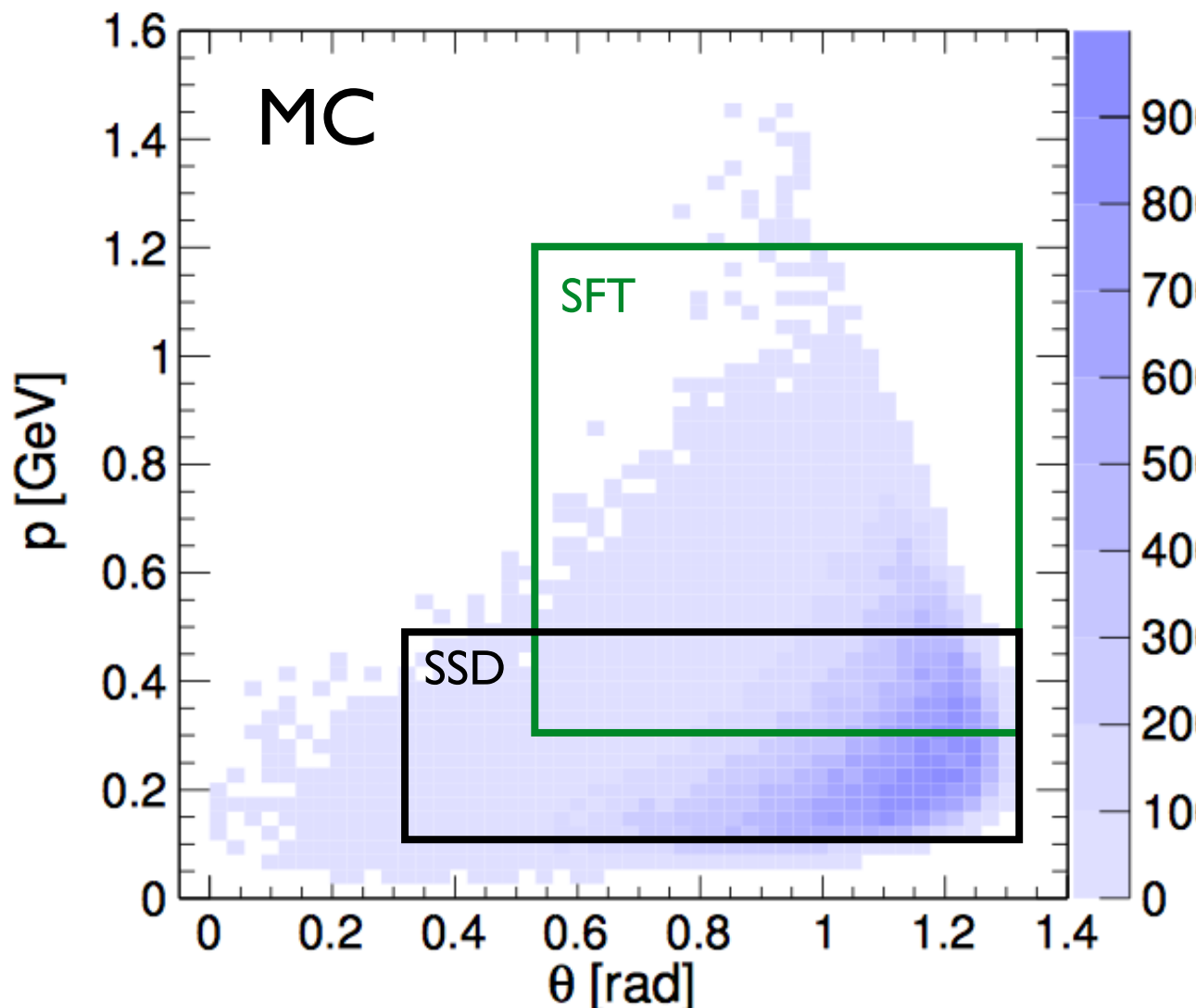


11.5 cm (18.5 cm) inner (outer) radius

1318+1320 (2198+2180) fibers with a diameter of 1 mm each

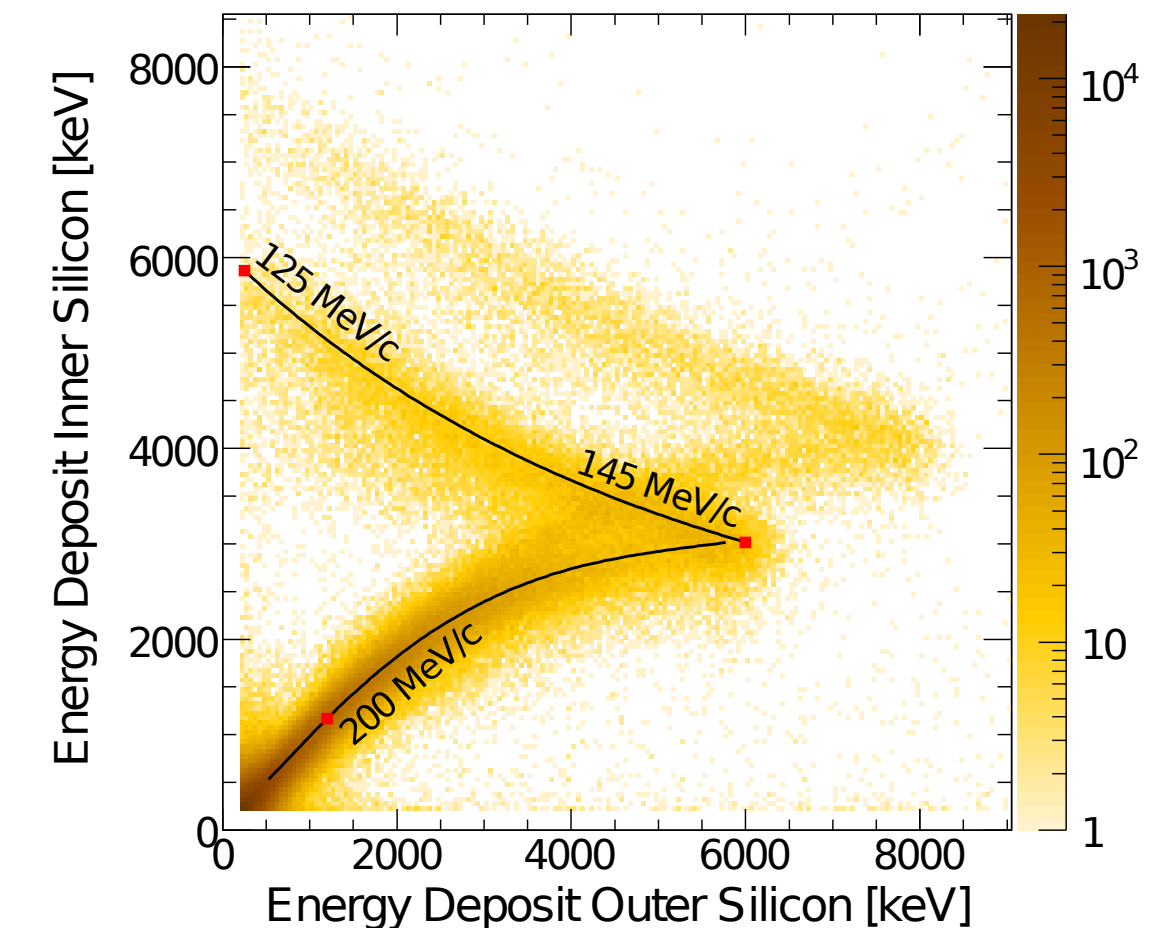
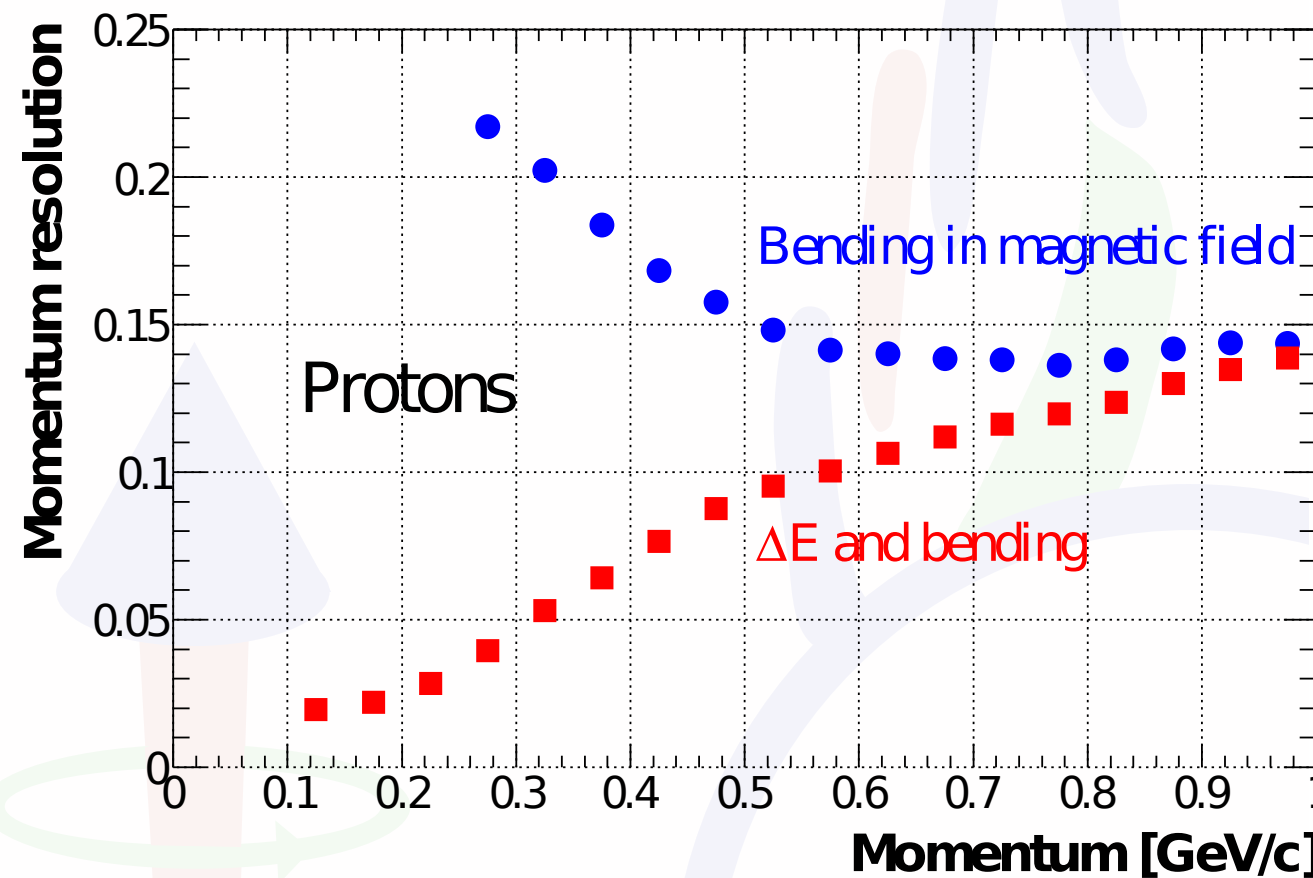
readout by 64-channel Hamamatsu H7546B MAPMTs

Kinematic coverage of the HERMES RD



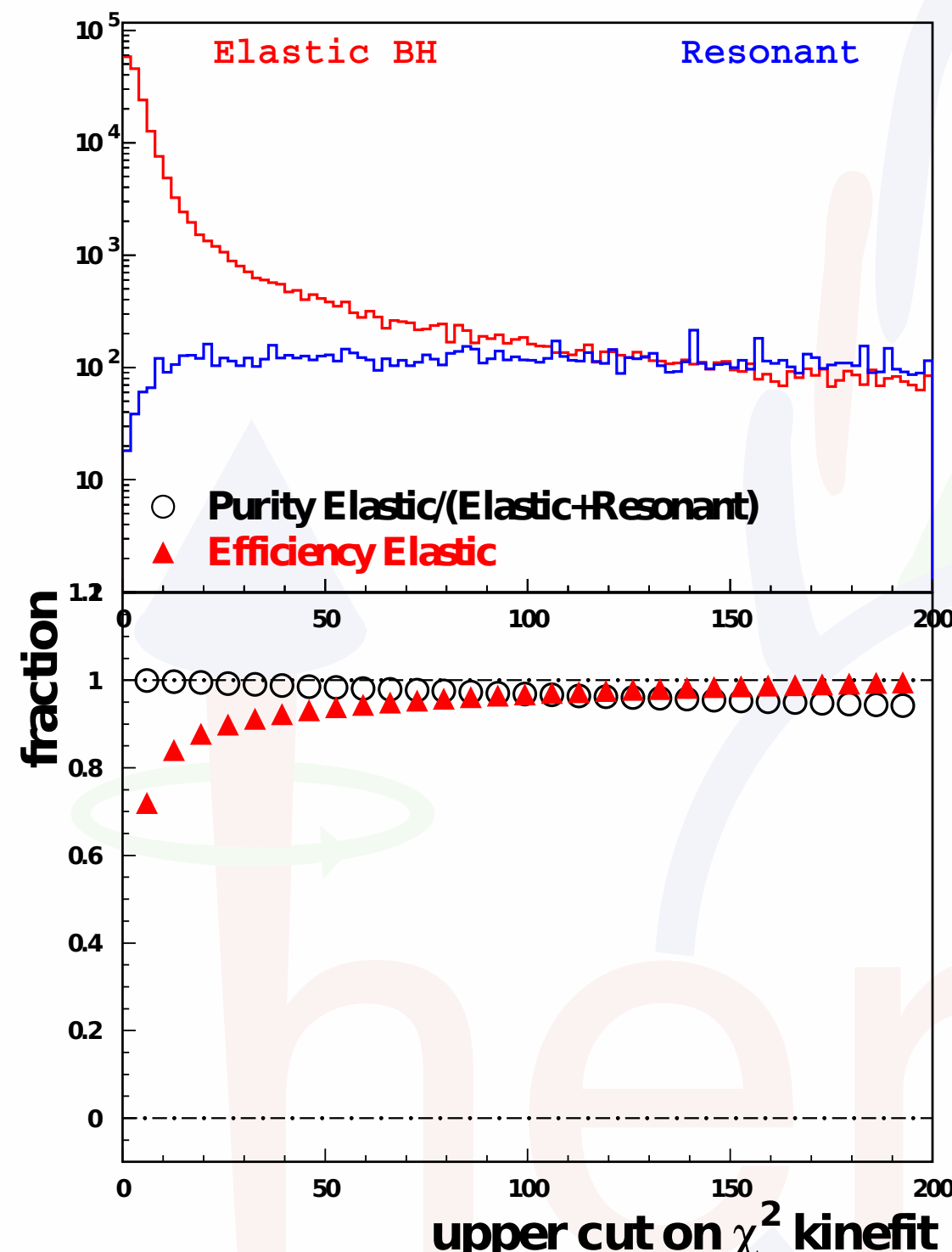
Scintillating fibre tracker (SFT) and silicon strip detector (SSD) complement each other

Recoil-detector tracking



taking energy loss into account improves momentum resolution for low p
azimuthal-angle resolution: 4 mrad
polar-angle resolution: 10 mrad (for $p > 0.5$ GeV)

Kinematic event fitting

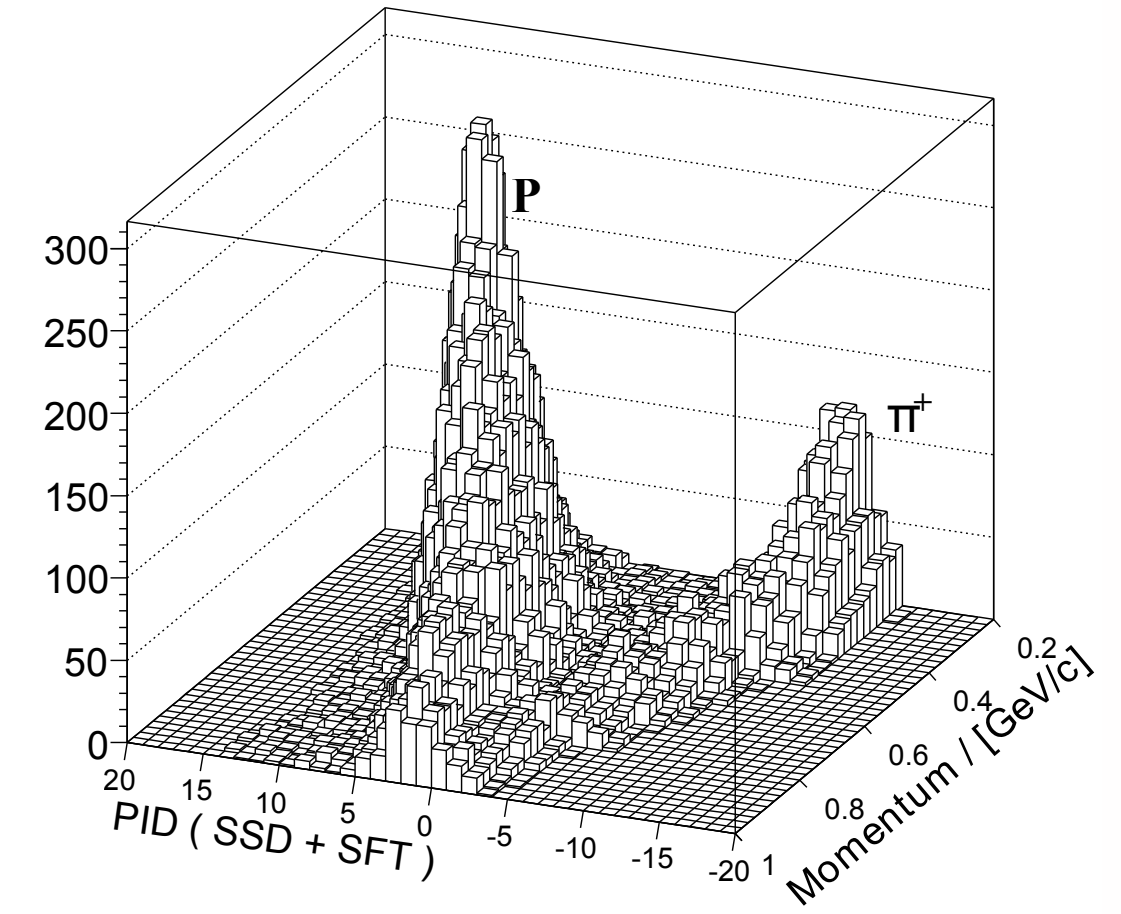
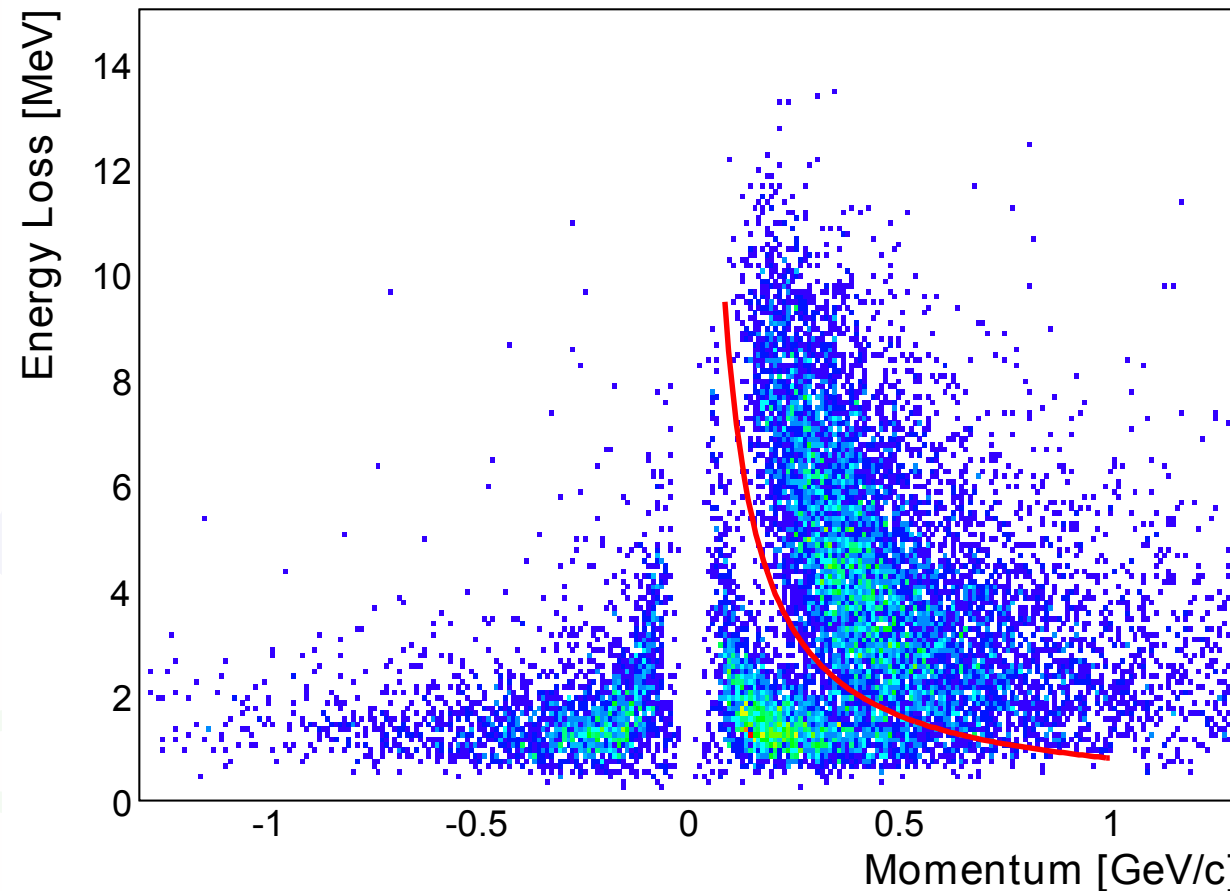


$$\chi^2_{pen} = \sum_{i=1}^9 \frac{(r_i^{fit} - r_i^{meas})^2}{\sigma_i^2} + T \cdot \sum_{j=1}^4 \frac{[f_j(r_1^{fit}, \dots, r_9^{fit})]^2}{(\sigma_j^f)^2}$$

χ^2 -value of interest penalty term constraints

- 4-momentum conservation as constraints
- lowest χ^2 -value in case of multiple recoil tracks per event
- minimum of 1 % fit probability required, which corresponds to $\chi^2 < 13.7$

Recoil PID

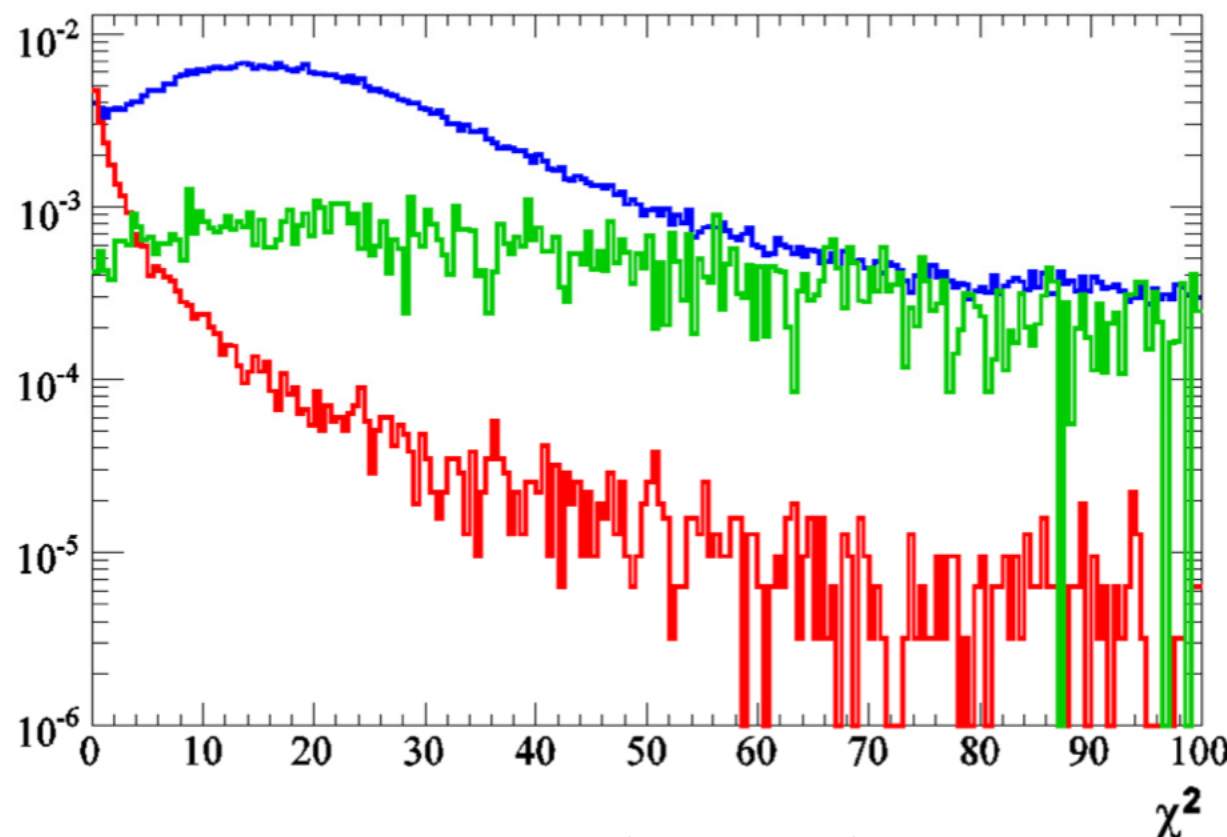


discrimination between protons and positively charged pions

parent distributions were crucial and determined experimentally

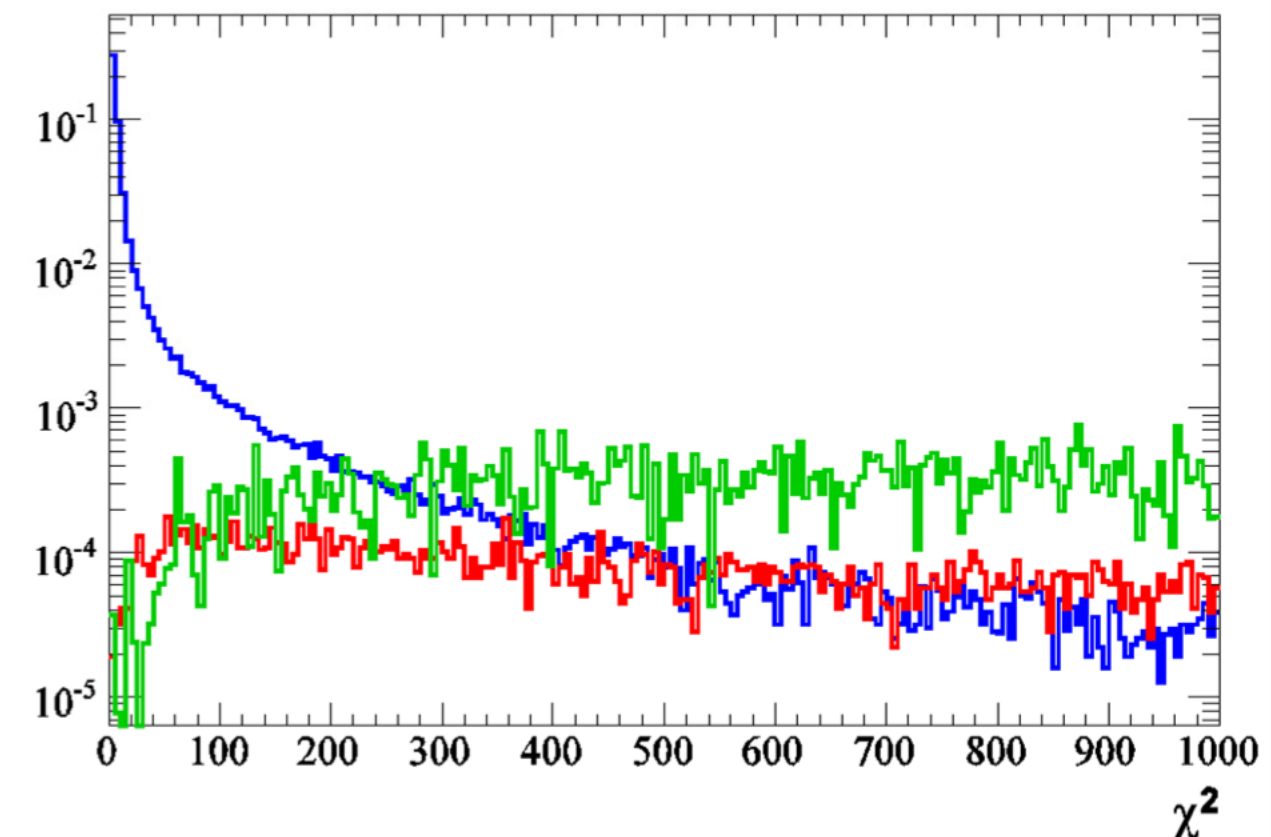
Kinematic fitting for $ep \rightarrow e\gamma p\pi^0$

$ep \rightarrow e\gamma p\pi^0$ $ep \rightarrow e\gamma p$ SIDIS



$ep \rightarrow e\gamma p\pi^0$ hypothesis

$$\chi^2_{ep \rightarrow e\gamma p\pi^0} < 4.6$$



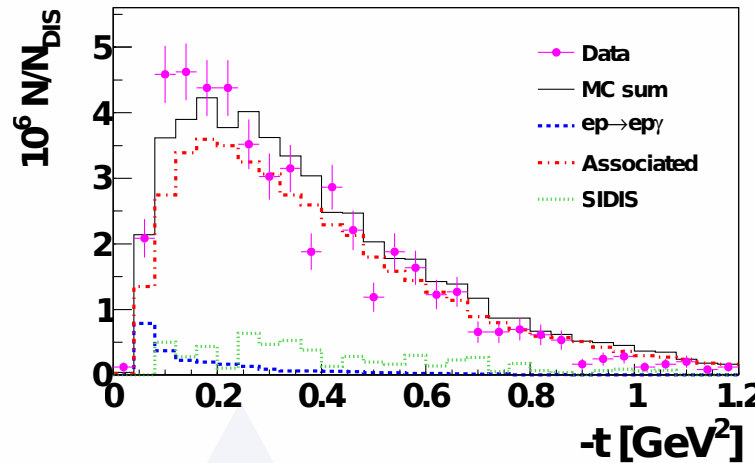
$ep \rightarrow e\gamma p$ hypothesis

$$\chi^2_{ep \rightarrow e\gamma p} > 50$$

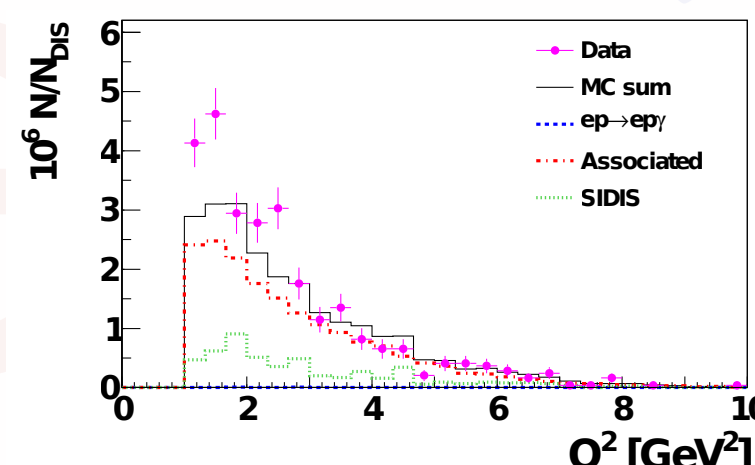
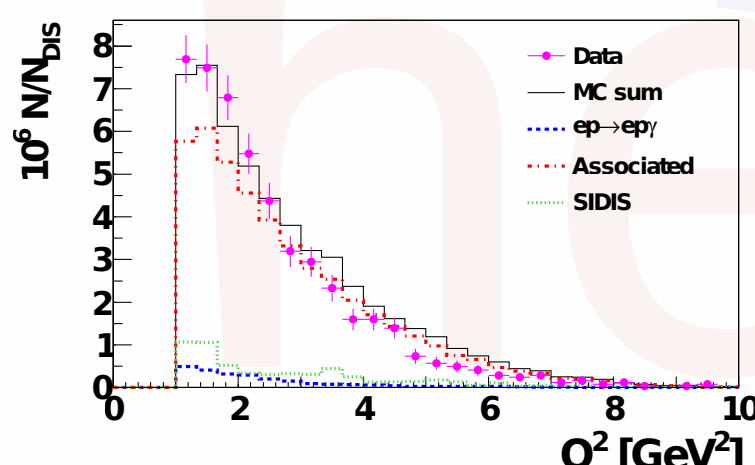
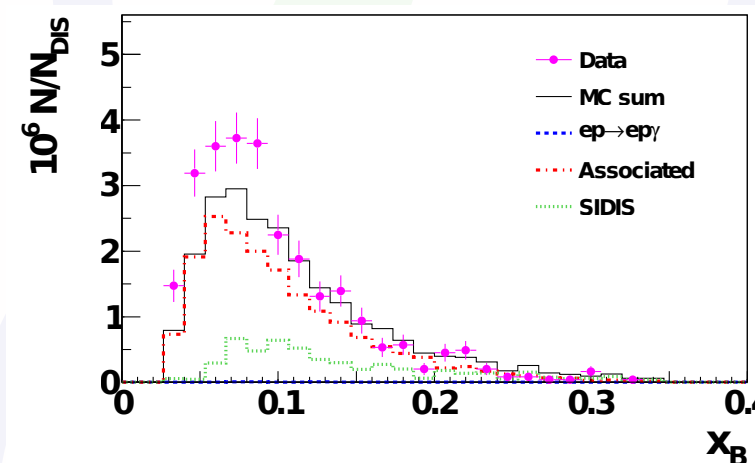
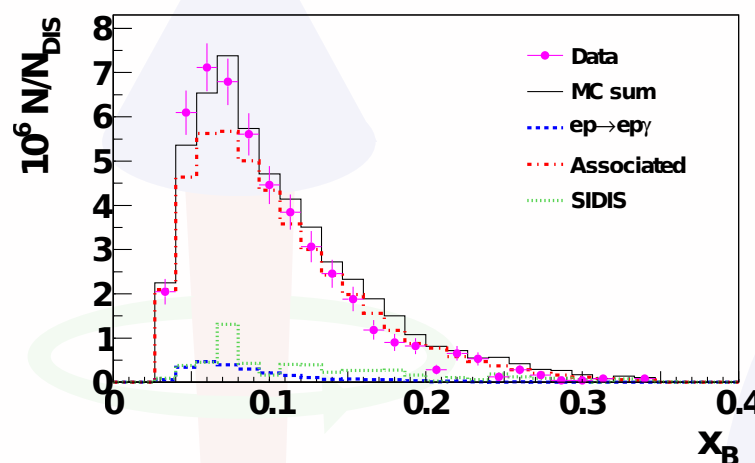
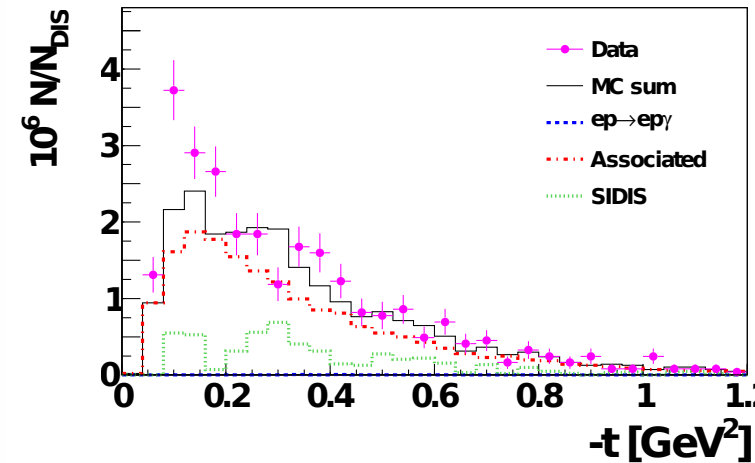
Using powerful kinematic fitting of $ep \rightarrow e\gamma p$ hypothesis
is crucial for the $ep \rightarrow e\gamma N\pi$ analysis

Selection of associated events

$ep \rightarrow e\gamma p\pi^0$



$ep \rightarrow e\gamma n\pi^+$



Uncharged particle
remains undetected

Kinematic fitting in case
of $ep \rightarrow e\gamma N\pi$ hypothesis
therefore not as strong

Additional selection criteria:

- Recoil PID information
- Lower-cut on $ep \rightarrow e\gamma p$ hypothesis